Mining, Metallurgy & Exploration
https://doi.org/10.1007/s42461-024-01128-6

# Paradox Basin Uranium-Vanadium Deposits: Comparative Mineralogy and Paragenesis

**Isabel Barton**[1] · **Mark Barton**[2,3]

Received: 20 December 2023 / Accepted: 16 October 2024


## Abstract

Broadly similar U(-V) deposits are hosted by Permian to Jurassic sandstones in the Paradox Basin of the Colorado Plateau. Common features of all the Paradox Basin deposits include occurrence in bleached red bed sandstones; accessory barite and/or celestine; authigenic Ti minerals; lack of correlation between mineralization and plant coal distribution; and evidence for or actual traces of hydrocarbons in the rock before and/or during mineralization. All but the structure-hosted Cutler deposits also show a mix of hematite, pyrite, and hypogene U and/or V minerals enclosed under authigenic overgrowths surrounding detrital quartz cores, which are extensively replaced by fringes of vanadian phyllosilicates. In the Entrada-hosted deposits, all but traces of hypogene U and V oxides have been removed to leave mainly the V-phyllosilicate minerals, but otherwise they resemble the mineralogy and paragenesis in the rest of the Paradox Basin U-V deposits. This paper presents and compares the deposit types to each other and to global sandstone-hosted U resources. Deposits hosted in the Jurassic Salt Wash Member of the Morrison Formation mostly form tabular, V-dominated bodies in permeable, trough cross-bedded horizons of bleached former red beds. Common quartz overgrowths entrap pyrite, pitchblende, and montroseite. Pitchblende and montroseite also form interstitial masses in cementing V-phyllosilicates, which corrode and partially replace the quartz overgrowths. Common accessory phases include pyrite (some framboidal), chalcopyrite, ferroselite, clausthalite, galena, sphalerite, and barite, with minor asphalt globules that corrode quartz overgrowths and cores and contain pitchblende and pyrite. Down the stratigraphic section, the Jurassic Entrada hosts minor lenticular deposits in aeolian sandstones just below a capping limestone. Ore minerals consist mainly of roscoelite replacing quartz overgrowths and cementing the sandstone. Except for small vanadiferous pitchblende inclusions trapped under quartz overgrowths, minor U-vanadates are the only U minerals observed. Continuing down-section, U-V deposits in the Triassic Chinle occur in conglomerates and sandstones just above the Chinle-Cutler unconformity in the Big Indian district, and in the basal Chinle in White Canyon. Quartz overgrowths are rarer but also enclose inclusions of hematite and pitchblende, more rarely V minerals. Pitchblende, montroseite, and V-phyllosilicates are the main ore minerals, forming interstitial masses and replacing some of the plant coal in the rocks. Accessory minerals include pyrite, sphalerite, galena, and barite. Secondary fluid inclusions fluoresce bright blue in ultraviolet light, indicating hydrocarbons. Chinle-hosted deposits in the San Rafael Swell occur as uraniferous asphalt that also contains V-Cr-Fe oxide. Roscoelite hosts most of the V and the deposits contain a large suite of accessory minerals, including pyrite, chalcopyrite, Ni-arsenide, sphalerite, galena, realgar, and barite. Where bleached, the coarse sandstone of the underlying Cutler Formation hosts small deposits below or near Chinle orebodies, either along permeable sandstones or along steep faults. Cutler-hosted deposits showing stratigraphic control share most features with the nearby Chinle orebodies, including quartz and rarer feldspar overgrowths enclosing U-V minerals and an assemblage dominated by pitchblende and montroseite with minor V-phyllosilicates. Deposits hosted along faults in the Cutler are highly distinct, mineralized with pitchblende and uraniferous asphalt in the fault cores and V-phyllosilicate in surrounding areas. Alone among the U and V deposits of the Paradox Basin, no quartz overgrowths have been observed in this type. Deposits' interpreted parageneses are also similar, with bleaching of original red beds during or shortly before the beginning of mineralization, followed by further U-V deposition in the main ore stage. Late in the ore stage, fresh V or V (hydr)oxide minerals back-reacted with silica in quartz overgrowths to form V-phyllosilicates, while accessory base metal sulfides and selenides precipitated along with barite. These similarities of mineralogy and texture imply a similar mechanism of formation for most of the Paradox Basin U-V deposits, corresponding either to a single basinwide ore-forming event or to the same geologic processes independently

Extended author information available on the last page of the article

Published online: 13 November 2024

repeated in different strata at different times. Hydrocarbons were likely a major reductant, with ore precipitating where an oxidized metal-bearing fluid either mixed with hydrocarbons or entered a rock previously reduced by their passage. Lastly, the Paradox Basin deposits' most remarkable feature is their high V content, which is unique worldwide and makes the area a world-class resource for this critical green energy metal.

**Keywords** Paradox Basin · Uranium · Vanadium · U-V deposits · Tabular uranium · Sandstone-hosted uranium

## 1 Introduction

Society's transition from fossil fuels to green energy sources is making uranium and vanadium supplies increasingly important. Uranium, mainly used for nuclear power, provides one of the lowest-$CO_2$ energy sources available on an industrial scale, and vanadium is required for emerging high-capacity batteries as well as for steel superalloys [1]. However, acquisition of both is likely to be precarious in future: uranium supply is listed as somewhat at risk, and vanadium supply as at extreme risk [2]. Accordingly, research into the geological resources available for future supplies is warranted, both by concerns over supply security and by the need to improve green energy availability.

### 1.1 Importance of Paradox Basin U-V

In the USA, among the most important resources of U and V are the sandstone-hosted deposits of the Paradox Basin, Colorado Plateau (Fig. 1). These supplied much of the US domestic U and V production over the twentieth century, including contributions to the Manhattan Project, Cold War energy security programs, and subsequent nuclear-power initiatives [3]. Sandstone-hosted deposits as a class have supplied the plurality of total global U production [4]. Far from being exhausted, the Paradox Basin deposits remain important among US reserves of U and V today [1]. Recent technological trends, such as research into the vanadium redox flow battery, have stimulated renewed interest in the Paradox Basin ores in the last decade. That combined with use in alloy steels and refinery catalysts has made V in particular a recurring feature of the American list of critical minerals, which are defined by the USGS as minerals that are economically crucial and whose supply is prone to interruptions [1]. The area is still home to numerous exploration and development efforts for U and V, as well as one U-V processing mill at White Mesa and two intermittently operating mines at Sunday (Gypsum Valley) and Pandora (La Sal) (Energy Fuels Inc. 10K report, 2020).

Besides their economic role, the Paradox Basin deposits are important scientifically. They represent a diversity of deposit subtypes not seen in other U- or V-bearing basins (Table 1). Alone among the world's sandstone-hosted U deposits, those of the Paradox Basin host major V resources, commonly with V in excess of the U endowment [1]. It was in the Paradox Basin that sandstone-hosted U was originally discovered and described, making it the type locality for what is now a globally recognized variety of ore deposit.

### 1.2 Background and Motivation for This Study

Despite the deposits' ongoing importance, the majority of the scientific work on the Paradox Basin U-V ores and related alteration dates from the 1950s–1960s [5]. When the uranium price collapsed in the 1970s, mining declined, and took geological and research interest with it. While publications on Paradox Basin U and V deposits continued to be produced into the 1990s, most relied on samples collected and fieldwork conducted years or decades earlier, and fieldwork diminished.

Much of the research done in the Cold War era was excellent in quality, with far better access and exposures than today. However, it was also limited by the analytical equipment available at the time and by the still-developing understanding of the Paradox Basin's geological history and context, the nature of U and V deposits, and the chemistry of both elements. Many of the technological and conceptual advances of the last 50 years have yet to be applied to the examination of the Paradox Basin U-V deposits, with the result that much remains unknown or uncertain about their geology and genesis.

Synthesis was also lacking. Though extensive, most of the twentieth-century work on the Paradox Basin U-V deposits focused on individual districts and/or deposit types, for example the Big Indian unconformity ores or the Slick Rock Salt Wash-hosted ores. There was surprisingly little effort at synthesis or comparison across deposit types, or at constructing a general theory of U and V deposition in the Paradox Basin. The few such attempts at synthesis were by Kerr [6] and Sanford [7–9]. Kerr tabulated and compared his observations from the Chinle-hosted mineralization in the San Rafael Swell and the structure-controlled mineralization in the Cutler to research by others on the Chinle-hosted ores, and to the U-bearing breccia pipes near Arizona's Grand Canyon, outside the Paradox Basin. Evaluating these

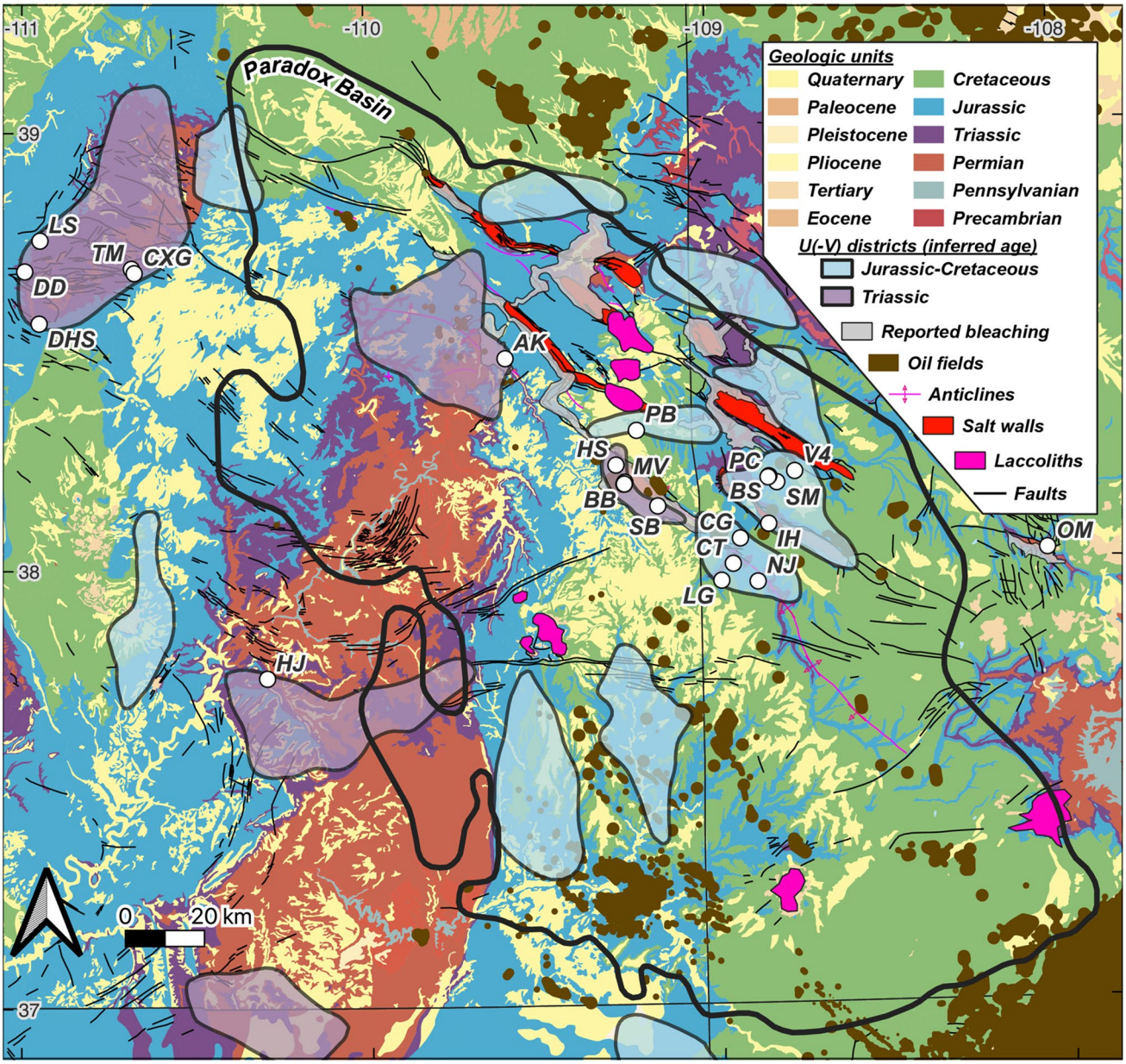


**Fig. 1** Generalized geologic map of the Paradox Basin with major U-V deposits and districts marked. *PB* Pandora/Beaver, *CG* Cougar Group, *NJ* Norma Jean, *LG* Legin Group, *CT* Charles T, *V4* Van #4, *SM* Schoolmarm, *IH* unnamed rim cut near Indian Henry's Cabin, *BS* Blue Streak, *PC* Picket Corral, *OM* Omega Group, *MV* Mi Vida, *BB* Big Buck, *SB* Serviceberry, *HS* Homestake, *HJ* Happy Jack, *TM* Temple Mountain, *CXG* Calyx Group, *DD* Dirty Devil, *DHS* Delta/Hidden Splendor, *LS* Lucky Strike, *AK* Atomic King, *BBC* Big Buck Cutler. Map courtesy of Eytan Bos Orent

deposits in light of the then-current metallogenetic theory, Kerr [6] settled on a hydrothermal formation process for the deposits related to structures and collapse features. His analysis omitted the large deposits in the Salt Wash and at the Chinle-Cutler unconformity at Big Indian. In contrast, these were the main foci of the second synthesis by Sanford [7], who attempted to model the fluid flow that created the U-V deposits. His simplified but innovative model found that the Salt Wash and Chinle (Big Indian) U-V deposits were associated with ascending groundwater flow paths, mainly in an upwelling zone on the edge of the impermeable Uncompaghre block where the permeable Jurassic aeolian sandstones become thinner. The cause of mineralization, he inferred, was the mixing of the ascending fluid with a local groundwater, though which carried the metals and which served as the reducing agent remained an open question. Sanford refined this model in two later papers [8, 9] for the Salt Wash U-V deposits, but did not include the

**Table 1** Summary of major geological characteristics of Paradox Basin U-V deposit types

| Deposit type | Host lithology | Deposit geometry | Relationship to stratigraphy and structure | Typical U-V ratio | Minor/accessory elements |
|---|---|---|---|---|---|
| Salt Wash | Quartzarenite | Tabular to complex rolls | Possible relationship to regional stress concentrations; variable occurrence in different sandstone "rims" | V > U | Pb, Se, Cu, Zn |
| Entrada | Quartzarenite | Lenticular | Occurrence controlled by limit of local Pony Express limestone; discordant to stratigraphy | V > > U | Cr, Se (?) |
| Chinle (Big Indian) | Coarse arkose | Tabular, bedded with discordant boundaries | Hosted at / near unconformable Cutler-Chinle contact | V > U to V ~ U | Cu, Zn, Pb, Mo |
| Chinle (San Rafael Swell) | Finer arkose | Tabular | Occurrence controlled by channel scours, highest grades along discontinuities | V > U | Cu, Zn, Pb, Cr, As |
| Cutler (stratigraphic) | Coarse arkose to fine conglomerate | Tabular, bedded with discordant boundaries | Hosted at / near unconformable Cutler-Chinle contact | V > U to V ~ U | Uncertain |
| Cutler (structural) | Variable clastic sediments | Vein | Hosted within or near high-angle normal faults | U > V | Sr, Cu, Pb, Mo, Zn |

Chinle-hosted unconformity or other deposit types. Similarly, a recent overview of U deposits in the Colorado Plateau as a whole focused on deposits hosted in the Chinle, Salt Wash, and Todilto Formations in the Grants Basin, using a relatively small number of mainly grab samples from each type examined by scanning electron microscopy [10]. Many of them were highly oxidized and/or provided secondhand, and thus lacked both original geologic context and unaltered hypogene minerals and textures.

Otherwise, there has been little or no effort at rigorous and detailed documentation, comparison, or synthesis of the multiple U-V deposits in the Paradox Basin. Therefore, the two goals of this study are (1) to document the ore and gangue mineralogy, textural relationships, and geochemical characteristics of the U-V deposits in the Paradox Basin in detail using modern observational and analytical techniques, and (2) to synthesize new and previous observations to compare the different deposit types within the Paradox Basin. Some of our observations have clear metallogenetic implications, but reevaluating deposit origins in full is a subject for a subsequent article. The present paper will focus on observational data, with limited exploration of their implications for metallogenesis.

### 1.3 Context of This Study

The present contribution offers a partial basis for an integrated study of the Paradox Basin mineral deposits and alteration, not only as subjects in themselves but also as manifestations of a larger Paradox Basin geological and geochemical history. After providing updated descriptions of the U-V deposits' mineralogy, textures, and paragenetic characteristics, we compare the deposit types across the basin and globally. The goal is to identify what, if anything, is unique about the Paradox Basin's metallogenetic and geologic history.

Most observations presented in this text are general and are consistent across multiple deposits of the type under discussion in a given subsection. Statements that apply to only one or a few deposits of a type, but not to others, are denoted by giving the names of the deposits.

## 2 Geological Background

### 2.1 Geologic Setting in the Paradox Basin

The Paradox Basin (Fig. 1) began forming around 315 Ma as a foreland basin associated with the Ancestral Rockies orogeny [11]. The outline of the basin sensu stricto is typically delineated by the maximum extent of evaporites in the Paradox Formation, a 2.5-km-thick mixture of Pennsylvanian black shales, evaporites, and carbonates deposited as the basin began forming [12]. Areas outside the perimeter of the salt contain thick sequences of Paradox Formation carbonate and clastic facies and lack

only the evaporites [11, 13]. Thus, fringing areas like the San Rafael Swell have been part of the Paradox Basin hydrologic system since the Pennsylvanian, but have not been subjected to the salt tectonic movement that started to define basin structure during the Permian [13]. Large-scale salt movement began as the voluminous, mostly red bed clastics of the Cutler Formation were deposited over the marine section [14] and continued periodically to the later Mesozoic through the deposition of Triassic fluvial and lacustrine, then Jurassic aeolian, fluvial, and lacustrine strata (Fig. 2). This created a series of northwest-trending salt walls that cut the lower to middle units of the modern basin. Lying over them are more reduced Cretaceous sandstones, conglomerates, and mudstones. Around 28 Ma, the basin was cut again by the intrusion the La Sal, Abajo, and Henry mountain laccoliths. Uplift and rapid incision followed across the region [15, 16]. More detailed accounts are given by Baars [17], Nuccio and Condon [18], Blakey and Ranney [19], and in the volume edited by Sprinkel et al. [20], among many others.

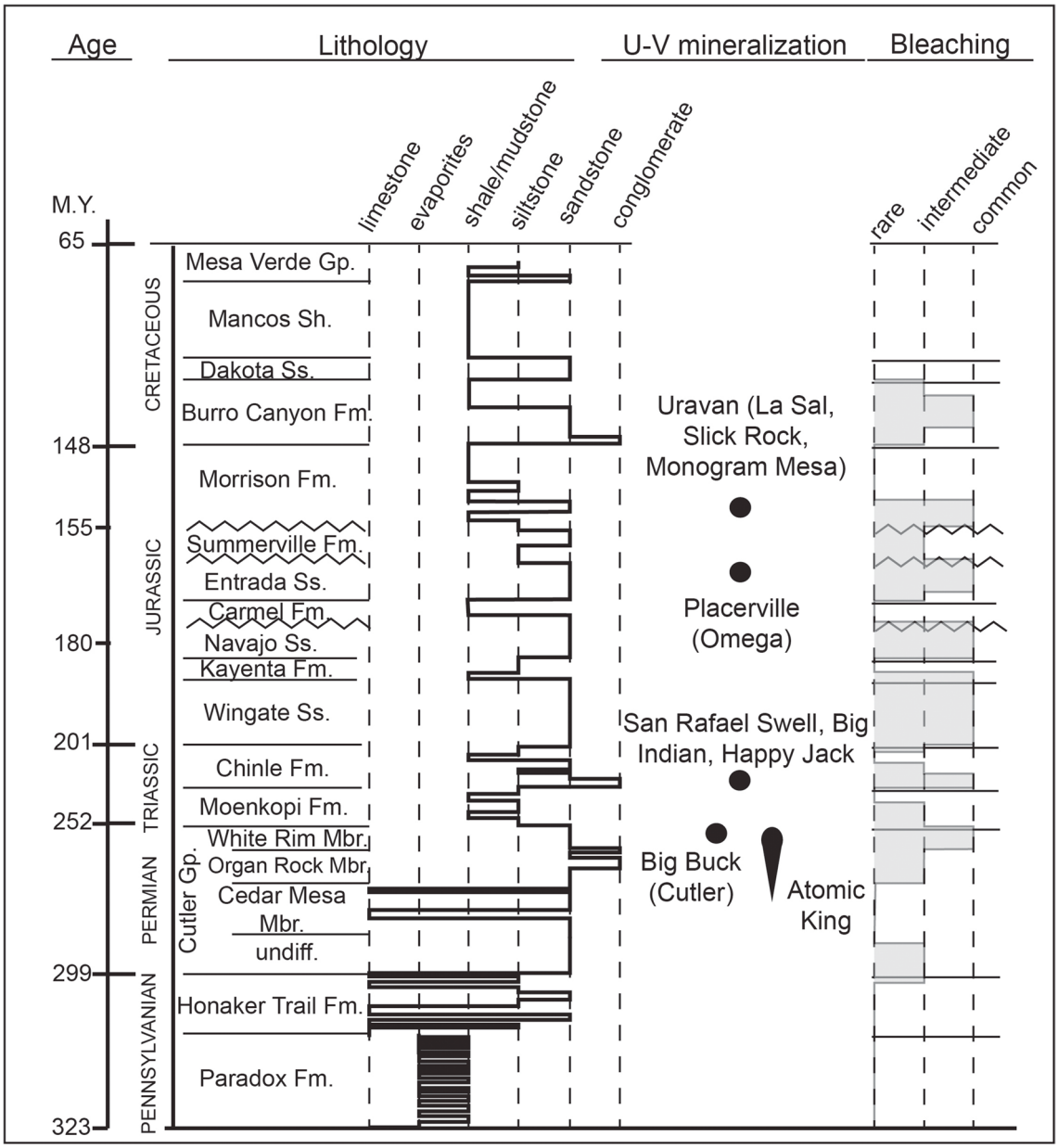


**Fig. 2** Generalized stratigraphic column of the Paradox Basin, showing bleached zones and stratigraphic horizons of U-V deposits covered in the text. See text for local variations and unconformities. (I.F. Barton, unpublished work)

As it evolved, the Paradox Basin probably hosted brines formed from highly evaporated paleo-seawater; brines formed from dissolution of evaporites in recharged meteoric water; fresh groundwater; oil and gas and associated oil-field brines; magmas; magmatic fluids; and $CO_2$-bearing fluids. Some of these are still present today [21]. Repeated and diverse fluid-rock reactions left numerous traces in the basin, such as hydrocarbon reservoirs (e.g., [22],extensive bleaching of redbeds [23–26],salt dissolution [27],and metal and mineral resources including Co, Mn, Cu, U, V, and potash concentrations.

### 2.2 Types and Geology of U-V Deposits

The Paradox Basin U-V deposits covered in this article fall into six distinct types based on host rock, orebody geometry, and/or location: (1) tabular U-V deposits hosted in the Salt Wash; (2) tabular V deposits in the Entrada in western Colorado; (3) U-V deposits in the basal Chinle just above an unconformity with the Cutler Formation in Big Indian; (4) sandstone-hosted U deposits in the lowermost Chinle in the San Rafael Swell, White Canyon, and elsewhere (variably associated with brecciated rock); (5) stratigraphically controlled U-V deposits in the uppermost Cutler; and (6) structurally controlled U-V deposits in the uppermost Cutler. Figure 1 shows the occurrences of each type of U-V deposit in the Paradox Basin. Table 1 compares their general characteristics, and Table 2 shows the deposits, types, and extents of access and sampling in this study.

### 2.3 Salt Wash Deposits

The most widely distributed U-V deposits are hosted in the fluvial sandstones of the lower, Salt Wash Member of the Jurassic Morrison Formation (Fig. 2). These have been extensively described, mapped, and interpreted by multiple contributors to the volume edited by Garrels and Larsen (1959), along with Carter and Gualtieri [28], Shawe [29–32], Northrop and Goldhaber [33], and Northrop et al. [34] among others. The ore-hosting Salt Wash Member of the Jurassic Morrison Formation was probably deposited in a rapidly evolving braided stream environment, likely on an alluvial fan [35]. The deposits occur in lenticular sandstones, normally pink but colored tan or white in and near mineralization [28]. The U-V deposits have a tabular to rollfront geometry with irregular shapes, typically parallel to crossbeds and other sedimentary structures [28]. In rare cases such as the Blue Streak mine, ore occurs as one continuous strip, subconcordant to stratigraphy and varying in thickness from about 30 cm to 1 m over several hundred meters' lateral distance. The four sandstone units commonly present in the Salt Wash may all host ore, although most deposits occur in one or more of the upper two sandstones. However, the exact stratigraphic position of many of the deposits is unclear (Craig Howell, Nuvemco, pers. comm., 2020. Ore-bearing channels may cut downward into underlying mudstone beds, forming sandstone- or conglomerate-filled scours up to 20 feet deep and commonly mineralized [28]. A dominant east–west orientation has been observed, but no clear relationship with flow patterns [36]. Mineralization typically occurs where the sandstone layers closely adjoin an overlying coarse fluvial conglomerate, with the highest grades occurring where the two are in direct contact and the usually intervening mudstone layer is absent [37]. Depending on scale, there can be some structural control along with the sedimentological localization. Except for a few minor fracture-controlled examples, structures do not localize mineralization at or below the deposit scale [35], but in the Slick Rock district deposits cluster around the Dolores zone, a northwest-trending band of moderately strong faulting aligned with the Lisbon Valley Fault to the northwest. Deposits are especially abundant where the zone is crosscut by a set of transverse faults [32]. Geochemical variations are common at multiple scales and tend not to correlate with any stratigraphic or structural features other than the Dolores zone. Although generally high V:U ratios are characteristic of Salt Wash-hosted tabular deposits, exact ratios vary from 1:1 to 20:1, without apparent connection to known mineralogical or geological factors [35, 38]. Deposits have no definite trend in V:U ratio with location or direction [39].

### 2.4 Entrada Deposits

The middle Jurassic Entrada Formation, below the Salt Wash, includes two to three members depending on location. In western Colorado, the lowest Dewey Bridge member consists of clay-rich siltstones and sandstones probably deposited in a coastal sabkha environment, just above the Chinle Formation [40, 41]. The overlying Slick Rock member is a thick sequence of crossbedded dune sandstones with generally high porosity and permeability. These were originally red, but have been bleached white on a regional scale by accumulation and migration of hydrocarbons and associated fluids [41]. The uppermost Moab Tongue sandstone is widespread in Utah but is absent in western Colorado, the only known place where the Entrada is mineralized. Fischer [40] mapped Entrada hosting marginal to subeconomic V(-Cr) enrichments near Rifle, Rico, Durango, and Placerville, and an anomalous Cr-rich clay accumulation in the Entrada east of Delta, CO. The majority of actual production was from the cliffs above Placerville, where small V-Cr deposits with accessory U were mined from 1910 to 1920 and intermittently thereafter until the early 1950s [40, 42],Barton, this volume). Clastic and diabase dikes are present in the area but their distribution is unrelated to the deposits', and they appear to be later features [43, 44]. Mineralization shows patterns related to stratigraphic rather than structural features.

**Table 2** Field sites visited during this study and described in the text. Locations of districts are marked in Fig. 1

| Deposit type | District | Mine / deposit | Location (WGS 84) | Exposure/access and sampling |
|---|---|---|---|---|
| Salt Wash-hosted (tabular to rollfront) | La Sal, UT | Pandora/Beaver | – 109.22028, 38.30944 | Active mine, sampled in situ |
| | Slick Rock, CO | Cougar Group | – 108.92624, 38.05917 | Reclaimed, dump samples only |
| | | Norma Jean | – 108.87788, 37.96 | Some ore exposed in remaining workings |
| | | Legin Group | – 108.98238, 37.9636 | Reclaimed, dump samples only |
| | | Charles T | – 108.94818, 38.00167 | Reclaimed, dump samples only |
| | Monogram Mesa, CO | Van #4 | – 108.76508, 38.21012 | Mine closed, stockpile sampled |
| | | Schoolmarm | – 108.81758, 38.18559 | Orebodies sampled in situ in decline |
| | | Unnamed rim cut near Indian Henry's cabin | – 108.84344, 38.09116 (approximate) | Ore exposed and sampled in old workings |
| | Greater Uravan, CO | Blue Streak | – 108.84000, 38.19944 | Ore exposed and sampled in mine workings |
| | | Picket Corral | – 108.84238, 38.19719 | Ore exposed and sampled in mine workings |
| Entrada-hosted | Placerville, CO | Omega Mine Group | – 108.04121, 38.0225 | Ore zones exposed near old workings, sampled in situ and on dumps |
| Chinle-hosted (Big Indian) | Big Indian, UT | Mi Vida | – 109.25652, 38.19166 | Dump and surface sampling (adit accessible but unsafe) |
| | | Big Buck | – 109.25929, 38.18719 | In-situ orebodies exposed in workings |
| | | Serviceberry | – 109.16259, 38.13609 | Reclaimed, dump samples only |
| | | Homestake | – 109.28129, 38.23109 | Reclaimed, dump samples only |
| | White Canyon, UT | Happy Jack | – 110.29347, 37.75254 | Adit accessible and sampled |
| Chinle-hosted (San Rafael Swell) | San Rafael Swell, UT | Temple Mountain | – 110.681, 38.69 (approximate) | Some ore zones exposed, but irregular; mainly dump samples |
| | | Calyx Group | – 110.67296, 38.67997 (approximate) | Not exposed, dump samples only |
| | | Dirty Devil | – 110.9913, 38.68441 | Inaccessible, dump samples only |
| | | Delta (Hidden Splendor) | – 110.94963, 38.56525 | Mainly inaccessible but some ore exposed outside workings; dumps also sampled |
| | | Lucky Strike | – 110.9469, 38.75487 | Some ore zones exposed, but irregular; mainly dump samples |
| Cutler-hosted structural | Kane Springs, UT | Atomic King | – 109.59737, 38.47804 | Limited ore exposed and accessible; in-situ and dump sampling |
| Cutler-hosted stratigraphic | Big Indian, UT | Big Buck (Cutler) | – 109.25819, 38.18749 | Inaccessible, dump samples only |

The Entrada is regionally extensive but hosts mineralization only around the depositional limit of the Pony Express limestone, a thin but impermeable layer that locally divides the Slick Rock sandstone into two beds [45]. Historical accounts describe the ores as forming lens-shaped bodies ranging from 1 to 2 in to 30 ft thick, with the highest grades concentrated along the lower edge of the possibly unconformable sandstone-limestone contact [42, 44]. Workings at Placerville reportedly extended more than 2000 ft horizontally, suggesting large-scale orebodies [46]. Orebody distribution appears conformable with bedding on a large scale, but in detail mineralization crosscuts lithologic boundaries [40, 45]. Most of the mineralization lies just below the unconformity, but Hess [44] documented several cases where ore minerals had apparently bled into the layers overlying the unconformity. Crosscutting the orebodies are thin bands of hard, unmineralized quartzite or silicified sandstone oriented parallel to the unconformity [44]. This quartzite is pale, whereas the V orebodies themselves are green to black

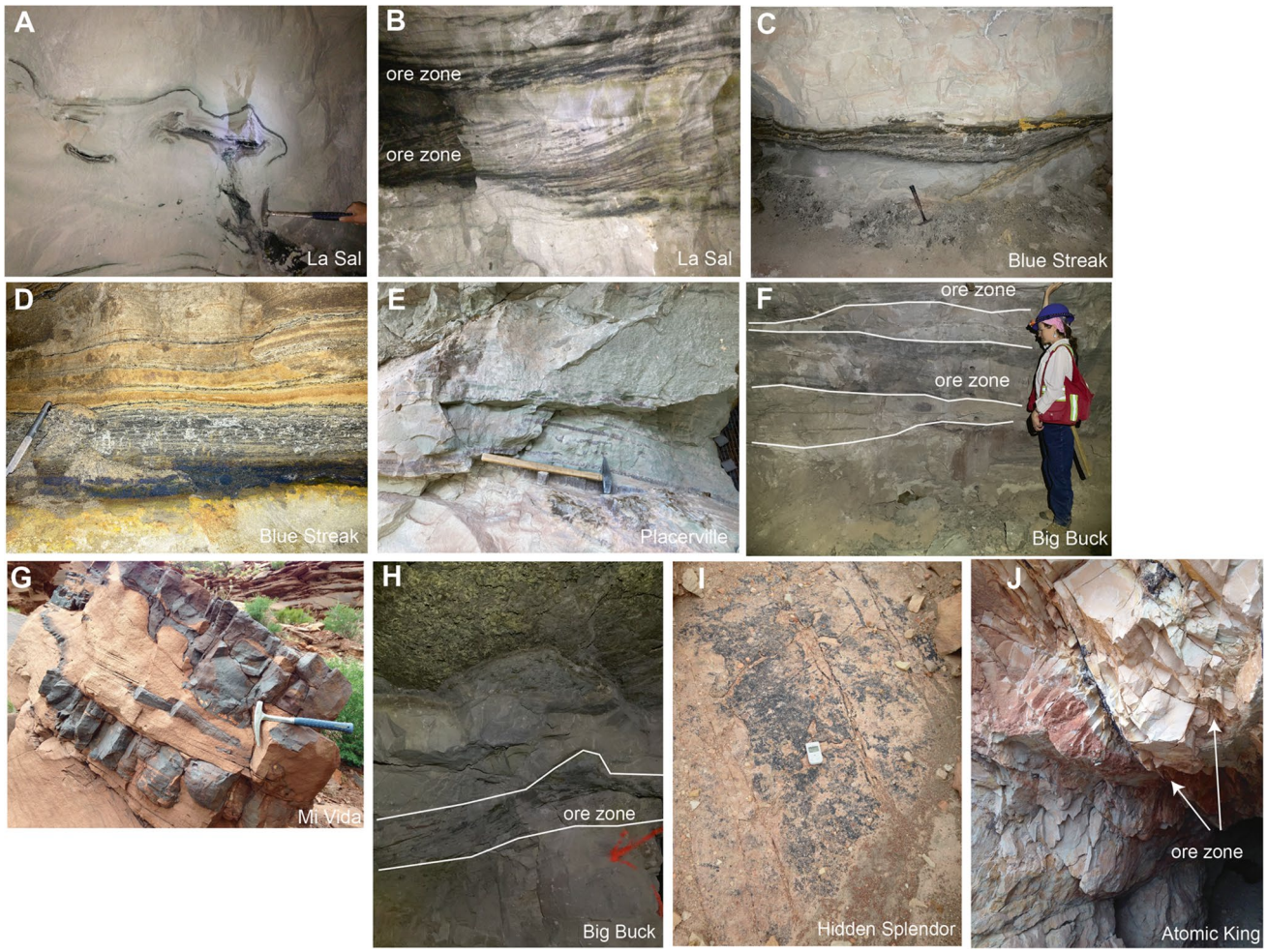


**Fig. 3** Ore zones and related alteration features around Paradox Basin U-V deposits. **A** Small Salt Wash-hosted orebody outcropping in the ribs of the La Sal mine. **B** Ore in trough cross-beds and coarse strata in the Salt Wash, La Sal mine. **C** The eponymous "blue streak" orebody exposed in a pillar in the Salt Wash-hosted Blue Streak mine. **D** Close-up of the "bacon rock" ore in the Blue Streak mine (see text for discussion). **E** Outcropping orebody of green V-phyllosilicates at the Omega mine, Placerville, CO. **F** Ore just above the Chinle-Cutler unconformity (lowermost white line) in the Big Buck (Chinle-hosted) mine, Big Indian district. **G** Hematite concretions in a red sandstone layer in the Chinle just outside the portal of the Mi Vida mine, Big Indian district. **H** U-V ore in a coarse lens exposed in a pillar in the Big Buck mine, Chinle Big Indian district, underneath unmineralized, pyritic coalified plant trash on the back of the mine. **I** Uraniferous asphalt ore exposed outside of the Hidden Splendor mine, Chinle San Rafael Swell. **J** Shoot of the ore zone at the structurally controlled Atomic King deposit in the Cutler Formation, Kane Springs district, consisting of mineralized asphalt in the central fault zone in bleached Cutler sandstone

(Fig. 3). Accessory Cr found as (probable) mariposite gives the Cr-rich, V-poor lower fringes of the northerly deposits a paler green shade, but is absent in the deposits nearest to Placerville [44]. Otherwise, no geochemical trends with distance have been reported. The Entrada deposits are noticeably U-poor, with the entire U resource reported in the literature consisting of minor carnotite staining.

## 2.5 Chinle Deposits (Big Indian and White Canyon)

The Triassic Chinle Formation hosts at least two types of U-V deposit. The largest and highest-grade are found primarily in the Big Indian district, on the flanks of the Lisbon Valley salt anticline, and in the White Canyon area on the west flank of the Monument upwarp (Fig. 1). At Lisbon Valley, deposits occur in the lowermost Shinarump member of the Chinle just above a low-angle unconformable contact with the uppermost member of the Permian Cutler Formation (the Moenkopi is missing in the area due to salt anticline movement in the early Triassic). In the White Canyon district, the deposits also occur in the Shinarump but are just above a low-angle unconformity with the Moenkopi, which is thin but present [47]. A second type of deposit in the Chinle occurs as stratabound ores not obviously related to unconformities or pinchouts. These are found in the San Rafael Swell, just outside the areal extent of the Paradox

evaporite facies but within the interpreted perimeter of its shale and carbonate layers [11, 48].

The ore-hosting Shinarump member of the Chinle is a fluvial arkosic sandstone to conglomerate, which Huber [49] identified as point bar deposits in Lisbon Valley and Miller [50] as an alluvial fan in White Canyon. Within these facies, the deposits in the southern end of the Big Indian district are confined to areas above the pinchout of a bed of Cutler sandstone, which is uniformly bleached and decemented near the ore zones. Its appearance has given this layer the common nickname "sugar sand" [51–53]. Locally, the sugar sand at Lisbon Valley contains remnant asphalt [54]. The angle of the unconformity ranges from a maximum of about 6° at the Big Buck mine to 2–4° northwest and southeast of it [55]. Above the unconformity, ores occur between the 6200′ and 6700′ structure contours on the top Cutler [51]. In the White Canyon district, the Moenkopi-Chinle unconformity is variable in position and angle and appears to have formed due to erosion by the Chinle fluvial facies [47]. Most mineralization is within 4–5 m above the Cutler-Chinle or Moenkopi-Chinle unconformity. Ore zones are directly above the unconformable contact with the uppermost Cutler or Moenkopi, or at most separated from the contact by a few feet of mudstone [47, 56]. Weir and Puffett [57] also documented a few cases in Big Indian in which mineralization extends down a few feet into the Cutler, and others in which the base of mineralization sits 30′ above the contact. They found that the unconformity controlled deposit locations in Big Indian, but no such clear relationship is documented from White Canyon. (In this paper, the Big Indian deposits will be termed unconformity-related while "Chinle-hosted sandstone deposits" will refer to deposits in both White Canyon and Big Indian.) The most important ore-hosting horizons in the basal Chinle are the channel or trough cross-beds, but mineralization is also reported in the finer-grained sheet sandstones that overlie multiple such scours [52].

Faulting, though common along all the anticlines, shows no spatial relationship to hypogene mineralization in any known deposit. Schmitt [58] mapped several instances where the Lisbon Valley Fault and associated smaller faults displace Chinle orebodies at Big Indian, and Trites and Chew [47] found that fracturing in Happy Jack probably postdated ore deposition there too. Subsequent studies failed to find any correlation between faults, fractures, and orebodies, or between orebodies and the thickness of the Chinle Formation or its members [47, 55].

Chinle-hosted orebodies are roughly concordant to strata but are irregular in shape, with sharp contacts between ore and barren rock [47, 55]. Orebody lengths in Big Indian range up to 10,000′ in length and 1400′ wide, with thickness variable but reaching 30′ at the large Mi Vida deposit [57]. White Canyon deposits are smaller, generally no more than 7′ thick and less than 1000′ long. The direction of elongation of the mineralized bodies at Big Indian is usually slightly transverse to the strike of the host beds [57]. Within mineralized zones and for feet to meters outside of them, the local Chinle is bleached from red to a gray-green shade. The color contact crosscuts stratigraphy and lithologic features. In zones of incomplete bleaching of the Chinle, notably in and outside the Big Buck mine, red conglomeratic clasts display green reaction rims. Massive hematite concretions, also discordant, are common in the tan to pink Chinle sandstones above the orebodies at Mi Vida and Big Buck. Despite being large, obvious, and abundant particularly outside the Mi Vida adit, they were only reported recently (Fig. 3g,[54]).

The distribution of U and V in the Big Indian deposits is somewhat erratic and the grades of the two metals do not correlate. Geochemical sampling and mapping by Kennedy [59] showed that the V:U ratio decreases to 0.04 to the northwest and downdip, from a maximum of 1.4 in the southeasternmost and updip deposits. Weir and Puffett [57] indicated that V minerals typically follow and are elongated in the direction of the local bedding planes, whereas U minerals are irregular in shape and commonly transverse to sedimentary structures. In addition, they described V minerals as occurring preferentially in finer-grained rocks with little calcite, in comparison to the mainly conglomerate- and sandstone-hosted U minerals typically found with abundant calcite. The relationship of ore to carbonized plant material in the mines is extremely inconsistent, with some plant coal localizing high-grade and other plant coal sitting unmineralized next to rich ore zones [47, 57]. Minor metals at Big Indian include Cu, Pb, Zn, and As. Ores at White Canyon differ from those at Big Indian mainly in lacking significant V. The main accessory metal there is Cu, and minor amounts of Pb, Zn, and As also occur within the deposits [47]. Copper as chalcopyrite is ubiquitous within U-mineralized zones and in haloes outside of them, ranging up to 40′ [50].

### 2.6 Chinle Deposits (San Rafael Swell)

The second major locus of Chinle-hosted U-V mineralization in the Paradox Basin is the San Rafael Swell, a large erosionally breached anticline west of Green River, UT on the fringe of the Paradox Basin, just beyond where the Paradox Formation salt pinches out (Fig. 1; [48]). There are reports of minor U(-V) occurrences in bleached formations from the Kaibab through the Navajo sandstone, but the Chinle is the only unit to carry significant U and V deposits, mainly in a belt along the southern edge of the Swell. Deposits, though mainly hosted in the Chinle, can extend short distances into the overlying Wingate Formation, typically with increasing V:U ratio going upward [60]. Orebodies are typically < 20′

thick and up to 600′ long, located in the lowermost 30′ of the Chinle in fluvial channel scours. Mineralization is exclusively present in sandstones, absent from intercalating lenses of mudstone [61]. Orebody geometry is generally tabular although a few rollfront and pipe-type deposits are reported [60]. The Chinle orebodies generally consist of pitchblende and related minerals finely disseminated within the asphalt abundantly filling host rock pores. Mineralization follows the asphalt along and across bedding.

Although channel scours localize the San Rafael Swell orebodies at a large scale, the distribution of mineralization within them is mostly fracture-controlled, as is the distribution of alteration [62]. Wright [63] describes a fault as localizing mineralization from the basal Chinle to the Wingate at mineable concentrations. Highest grades are found in shear zones, fractures, faults, and along bedding planes [60]. A possible larger-scale control by collapse features is debated. Several deposits occur along the flanks of collapse features or breccia pipes common in the area where large blocks of strongly bleached Glen Canyon Group sandstones have been dropped into strongly brecciated, deformed, and altered lower Chinle or even deeper. The collapse features' extent varies with occurrences but can range through 1500 ft of stratigraphy, with minor brecciation on the flanks of the structures [64]. Asphalt is ubiquitous in the sandstones in and around these collapse features, but is also quite common throughout the San Rafael Swell and may not be related to the collapses. The asphalt contains appreciable U and V around only a few of them, but also commonly carries U-V mineralization in fractures that are well away from them [64]. Based on their analysis, Kerr et al. [64] concluded that the San Rafael Swell U-V are unrelated to the collapse features, though Hawley et al. [60] contended that the two were linked.

A notable feature of the San Rafael Swell is the bleaching of ordinarily red rocks through a large swath of the stratigraphic section, from the Moenkopi to the Glen Canyon group inclusive [60]. While bleaching of redbeds is a common feature among all deposit types, at the San Rafael Swell the bleaching is uncommonly extensive and pervasive. Compared to other deposit types, bleaching in the Swell is also much more obviously related to hydrocarbons, which are still present in many of the bleached rocks. Bleaching also removed Fe more thoroughly than usual. Where most Colorado Plateau bleaching leaves 2 to 4% $Fe_2O_3$ in the rock, chemical analyses from the San Rafael Swell show roughly 1 to 2% $Fe_2O_3$ [60]. The rocks are bleached mainly at the higher parts of the Swell, red below them. Bleaching alteration decreased chlorite and feldspar, increased kaolinite and montmorillonite contents, and introduced barite, hematite, carbonates, jasperoid, and a variably uraniferous asphalt [60]. Bleaching removed Mg, Fe, Ca, and carbonate from the basal Chinle and lower strata, and added them to the upper Chinle and Wingate [64, 65]. As with other U-V deposits in the Paradox Basin, the ores occur exclusively in the bleached rocks, though not all bleached rocks are mineralized.

### 2.7 Cutler-Hosted (Stratigraphic Control)

The lowermost deposits on the Colorado Plateau are two types of U-V occurrences in the uppermost sandstone of the Permian Cutler Formation. Like the Entrada-hosted mineralization, these tend to be afterthoughts among the Paradox Basin U-V deposits. Some have been mined, but most pale in comparison to the resources hosted in the Chinle and Salt Wash. But mines in Cutler-hosted U-V deposits, such as the Small Fry mine in the Big Indian district, were among the first to be exploited in the postwar era, and roughly a dozen deposits were known by the later 1950s [56, 59, 66]. The discovery of Mi Vida and the other larger, richer Chinle-hosted orebodies in the same district finished them off. After 1954, no more ore was produced from Cutler deposits at Big Indian [57]. Since the 1980s, there has been little research on the Cutler-hosted U-V deposits of either type in the Paradox Basin.

The type found in the Big Indian district is stratigraphically controlled. Deposits occur in the bleached uppermost Cutler updip and northeast of the belt of Chinle-hosted deposits, mainly in areas where the basal Chinle sandstone is missing [52, 57, 67, 68]. Orebodies consist of lenses up to 600 ft long and 28 ft wide [56, 57, 63]. Even at a small scale, there is little evidence for structural control. While Isachsen [56] noted a correlation between joints and high-grade U-V ores, Weir and Puffett [57] were unable to substantiate this and inferred that the jointing was post-ore. This was supported by earlier observations by Jacobs [69], who found that the main control on the occurrence of Cutler U-V mineralization was the variable permeability of the upper Cutler lithologies. Campbell and Steele-Mallory [67] pointed out that as with the Big Indian Chinle-hosted deposits, the occurrence patterns of U and V within the Cutler deposits appear largely independent of each other and uncorrelated.

There is no observed difference between mineralized and barren sandstones in the Cutler, except for the metal grades and the lower abundance of carbonate cement in the ore zones [67]. Reynolds et al. [68] suggested that a pre-ore carbonate had been largely replaced by ore minerals in high-grade zones. Reported average grades are low, around 0.2–0.4% $U_3O_8$ and 0.3–0.7% $V_2O_5$ with V:U ratios varying from 1:1 to 7:1 [57, 70]. A small but consistent Cu content in the Big Indian Cutler-hosted U-V ores was reported by Johnson and Thordarson [35] and is consistent with the numerous reports of supergene Cu minerals at Cutler U-V deposits [57, 59, 66]. Listed mineralogy is pitchblende,

montroseite, doloresite, and a V-phyllosilicate described as either a V-clay or a V-illite [70].

### 2.8 Cutler-Hosted (Structural Control)

The second type of Cutler-hosted deposit occurs along structures, typically high-angle normal faults around which the normally red sandstones are bleached gray-green or white. Bleached zones around smaller fractures associated with the main faults can also carry mineralization [71]. The bleaching alteration consists of major iron depletion with extensive alteration of clay minerals from illite to kaolinite, hydromica, Fe-chlorite, and montmorillonite [72]. Remnant asphalt is common in the faults, and the bleaching is commonly attributed to the faults piercing reservoirs of oil, gas, or reduced waters along anticlinal crests [72]. This preparation, and the permeability provided by the fault, allowed U and V to be trapped from subsequent incoming solutions in any bleached and permeable stratum along the way. Wright [63] records that at the Atomic King deposit, not only the Cutler but the Moenkopi and Chinle Formations contain pitchblende mineralization. Mineralization generally consists of uraninite and vanadium clays, associated with calcite, pyrite, ankerite, and copper sulfides [71]. In contrast to most of the other U-V deposits known in the Paradox Basin, montroseite is rare, microscopic, and mostly developed along V-phyllosilicate cleavages. The V resource of the structure-related Cutler deposits appears to consist almost entirely of V incorporated in mixed-layer clays [72].

In addition to these major deposit types and districts, the Salt Wash in Gypsum Valley and the Chinle along the Moab Fault also host numerous, typically small, U-V-Cu deposits. These have seen small-scale and sporadic historical mining, but have barely been studied at all and remediation has severely limited the available mapping and sampling opportunities today. The Colorado Plateau region also hosts breccia-pipe U deposits, particularly in northern Arizona, but these are outside the main Paradox Basin area. The U-V-Cu and breccia pipe deposits are not covered in this article.

## 3 Materials and Methods

The principal fieldwork was conducted during the summers of 2015–2022. Where feasible, we visited ore deposits in situ and recorded location, lithological, textural, and field information. Where mines were inaccessible or reclaimed, we took samples from float, dumps, or remaining stockpiles. The sites visited and levels of available access and examination are in Table 2. Samples were made into polished thin sections and were examined by Nikon LV100POL petrographic microscope in transmitted and reflected light. A subset was analyzed in greater detail with a JEOL 6010LA benchtop scanning electron microscope (SEM) equipped with a Bruker EDS and Gatan MonoCL4 cathodoluminescence detector, and with a Cameca SX100 electron probe microanalyzer at the University of Arizona. Electron microprobe standards and operating conditions for each type of mineral analyzed are given in the Appendix.

### 3.1 Petrography of the Paradox Basin U-V Deposits

Table 3 summarizes the ore and gangue mineralogy of the Paradox Basin U-V deposits described in this section. Formulae of minerals mentioned in the text are in Table 4.

### 3.2 Salt Wash Deposits

#### 3.2.1 Detrital

Quartz is the main detrital phase in all Salt Wash deposits examined and makes up an estimated > 90% of the clasts. Euhedral overgrowths are very common in mineralized rocks and in nearby altered but unmineralized samples. A few claystone clasts are present in some of the rocks, but are rare. Albite- and tartan-twinned feldspars are relatively common, but SEM analysis shows potassic compositions dominate, even in grains with pronounced albite twinning. Muscovite and biotite clasts are noticeable for their absence, not being observed in any sample from Salt Wash-hosted U-V deposits. Detrital zircon is rare but present; other heavy detrital minerals are rare to absent, though some rutile habit and occurrence suggest pseudomorphing. Plant coal is present but not common and has a clear cellular texture.

#### 3.2.2 Alteration

Quartz overgrowths are ubiquitous, particularly in high-grade samples. Between overgrowth and detrital core are lines of minuscule (micron-scale) inclusions (Fig. 4e, H), identified by SEM as pitchblende, montroseite, U-V oxide, rutile, Ti-V oxide, pyrite, apatite, barite, and hematite in various samples and sites (Table 5). At Monogram Mesa, quartz grains with double overgrowths were observed to contain hematite inclusions below the inner, and pitchblende inclusions below the outer, overgrowth (Fig. 4). Suturing between quartz grains is also common, and sutures cross-cut overgrowths. The overgrowths are euhedral where they occur adjacent to open pores; are heavily corroded where they are in contact with vanadian phyllosilicates or base metal sulfides; and are almost skeletonized where they are in contact with asphalt globules (Fig. 4F, G). Overgrowths around K-feldspar are rare but can be found enclosing lines of hematite inclusions, typically in unmineralized or poorly mineralized samples. Previous work reported that the quartz

**Table 3** Mineralogy of Paradox Basin U-V deposits. *Italics* = previously reported but not observed in this study

| Mineral group | Deposit type | | | | | |
|---|---|---|---|---|---|---|
| | Salt Wash | Entrada | Chinle Big Indian | Chinle San Rafael Swell | Cutler stratigraphic | Cutler structural |
| Detritals | Quartz, K-feldspar, claystone, zircon, plant coal, lithics | Quartz, K-feldspar, calcite, rare muscovite, ilmenite, lithics | Quartz, K-feldspar, phengite, biotite, micrite, lithics, plant coal, zircon | Quartz, K-feldspar, phengite, biotite, zircon, chromite, micrite, chalcedony, lithics | Quartz, K-feldspar, albite, biotite, lithics, phengite, zircon, *tourmaline, apatite* | Quartz, K-feldspar, muscovite, biotite, ilmenite, monazite, zircon, *magnetite, chlorite, tourmaline,* lithics |
| Hypogene U | Pitchblende, U-V oxide | Vanadiferous pitchblende (inclusions) | Pitchblende, U-V oxide, U in montroseite | Pitchblende, U-V oxide | Pitchblende | Pitchblende |
| Hypogene V | Montroseite, U-V oxide, paramontroseite, *roscoelite*, V-illite, V-chlorite, corvusite, doloresite, duttonite | Roscoelite; possible evidence for montroseite pseudomorphed by hematite | Montroseite, U-V oxide, V-chlorite, V-biotite, roscoelite | V-Cr-Fe oxide, V-phengite with minor Cr | Montroseite, doloresite, V-Ti oxide, V-chlorite, V-illite or V-clay | V-clays, rare montroseite |
| Hypogene accessory metallic | Pyrite, chalcopyrite, chalcocite, covellite, galena, ferroselite, *eucairite*, clausthalite, *molybdenite, native Se*, sphalerite, *acanthite* | Pyrite, *mariposite* | Pyrite, high-Cd sphalerite, galena, chalcopyrite, *marcasite,* digenite, covellite, *molybdenite, jordisite*, chalcocite, *native Cu* | Pyrite, marcasite, chalcopyrite, *cattierite,* bornite, ferroselite, sphalerite, galena, realgar, Ni-arsenide, *native As* | Pyrite | Pyrite, chalcopyrite, galena, digenite, covellite*, molybdenite, sphalerite* |
| Alteration minerals | Quartz overgrowths, calcite, apatite, dolomite, barite, clay, gypsum, rutile, asphalt | Quartz overgrowths, barite, fluorapatite, rutile, (Mg-)calcite | Quartz overgrowths, illite, kaolinite, mixed-layer clay, rutile, monazite, fluorapatite, barite, celestine, calcite, albite | Quartz overgrowths, K-feldspar, asphalt, dolomite, kaolinitic clay, chalcedony, mixed-layer clay or zeolite, barite, Cl-rich apatite, monazite | Quartz overgrowths, albite, calcite, Fe- and K-Mg chlorite / smectite, zircon, rutile, fluorapatite, gypsum | Calcite, dolomite, kaolinite, (celesto)barite, gypsum, Al-Sr phosphate, rutile, asphalt |
| Petroleum | U-V-mineralized asphalt | Pyrobitumen(?); not definitively identified | Secondary fluid inclusions fluoresce blue | U-V-mineralized asphalt | *Organic carbon, undifferentiated* | Pyrobitumen observed; *reportedly mineralized* |
| Supergene minerals | Carnotite, tyuyamunite, andersonite, malachite, azurite, volborthite, metahewettite, others | Carnotite-tyuyamunite mixtures, hematite, other vanadates | Metatyuyamunite, tyuyamunite, carnotite, melanovanadite, malachite, others | Hematite, U-phosphate, tyuyamunite, carnotite, jarosite, other vanadates | Hematite | Andersonite, hematite, tyuyamunite, carnotite, other vanadates |
| Sources | [32, 36, 38, 73–78], this study | [40, 44–46, 79–82], this study | [57–59, 66, 83], this study | [60, 84–89], this study | [67, 68, 70], this study | [71, 72, 76, 90, 91], this study |

**Table 4** Formulae of minerals mentioned in the text

| | | |
|---|---|---|
| achavalite, FeSe | dolomite, $CaMg(CO_3)_2$ | mottramite, $PbCuVO_4OH$ |
| ankerite, $CaFe(CO_3)_2$ | doloresite, $V_3O_4(OH)_4$ | ningyoite, $CaU(PO_4)_2$ |
| azurite, $Cu_3(CO_3)_2(OH)_2$ | duttonite, $VO(OH)_2$ | paramontroseite, $VO_2$ |
| barite, $BaSO_4$ | enargite, $Cu_3AsS_4$ | pyrite, $FeS_2$ |
| biotite, $K(Fe,Mg)_3[AlSi_3]O_{10}(OH)_2$ | fluorapatite, $Ca_5(PO_4)_3F$ | pyrolusite, $MnO_2$ |
| bornite, $Cu_5FeS_4$ | galena, PbS | roscoelite, $K(V,Al)_2[AlSi_3O_{10}](OH)_2$ |
| brannerite, $UTi_2O_6$ | greenockite, CdS | rutherfordine, $UO_2CO_3$ |
| calcite, $CaCO_3$ | hematite, $Fe_2O_3$ | rutile, $TiO_2$ |
| carnotite, $K(UO_2)_2(VO_4)_2 \bullet 3H_2O$ | illite, $K_{0.65}Al_2[Al_{0.65}Si_{3.35}]O_{10}(OH)_2$ | tangeite, $CaCu(VO_4)OH$ |
| cattierite, $(Co,Fe,Ni)S_2$ | ilmenite, $FeTiO_3$ | tivanite, $VTiO_3(OH)$ |
| celestine, $SrSO_4$ | jarosite, $KFe_3(SO_4)_2(OH)_6$ | tyuyamunite, $Ca(UO_2)_2(VO_4)_2 \bullet 6H_2O$ |
| chalcocite, $Cu_2S$ | kaolinite, $Al_2Si_2O_5(OH)_4$ | uraninite, $UO_2$ |
| chalcopyrite, $CuFeS_2$ | lyonsite, $Cu_3Fe_4(VO_4)_6$ | uranophane, $Ca(UO_2)_2(Si_3OH)_2 \bullet 5H_2O$ |
| coffinite, $USiO_4 \bullet nH_2O$ | magnetite, $Fe_3O_4$ | uvanite, $U_2V_6O_{21} \bullet 15H_2O$ |
| covellite, CuS | malachite, $Cu_2CO_3(OH)_2$ | vesignieite, $BaCu_3(VO_4)_2(OH)_2$ |
| cryptomelane, $KMn_8O_{16}$ | montmorillonite, $(Na,Ca)_{0.33}(Al,Mg)_2Si_4O_{10}(OH)_2 \bullet nH_2O$ | volborthite, $Cu_3(V_2O_7)(OH)_2 \bullet 2H_2O$ |
| digenite, $Cu_9S_5$ | montroseite, (V,Fe)OOH | |

overgrowths are extremely abundant in mineralized intervals and rare outside of them [33], and that they preserved inclusions of montroseite, pyrite, and coffinite [32, 33, 92].

Carbonate and variably vanadian clay form the principal cements to the rock, with an antithetical relationship: carbonate dominates in the clay-poor areas and clay-rich areas contain little carbonate. Where both are present together, the carbonates overgrow the clay. The carbonate is most abundant in low-grade or unmineralized rocks, and tends to be coarse and sparry, in some places fibrous or rhombic. In all samples where both carbonates and quartz overgrowths occur, the carbonate is invariably outside the quartz overgrowth. Multiple types of carbonate were detected, including a relatively pure calcite and a dolomite with minor Mn and variable Fe. In general, the Fe content of the dolomite is under 0.5 mass %. Archbold [93] determined that the abundance of carbonate in Salt Wash ore deposits does not correlate with grade or mineralization, a conclusion supported by our observations.

The clay overgrows quartz, with extremely ragged contacts between clay and the remaining, typically partial, overgrowth silica. It is highly abundant in most rocks, and in ore zones is commonly the major V mineral. Where not vanadian, it is colorless and has a kaolinitic to illitic composition with no Mg or Fe detected. The clay contains inclusions of pyrite and is overgrown by gypsum in a few samples, and by carbonate where present.

Barite forms rare crystals that locally surround quartz overgrowths and clays and are Sr-poor based on EDS analysis. In samples from the Legin mine group in Slick Rock, barite concretions were observed as large crystals cementing the rocks. At La Sal, barite is overgrown by pyrite, montroseite, and asphalt, and forms inclusions in the vanadian phyllosilicates. Where in contact with pyrite, the barite has corroded edges. Gypsum is quite rare. It was observed in one sample from the Van #4 mine at Monogram Mesa, as large sparry crystals surrounding detrital grains, pyrite, and clay, and at a nearby unnamed rim cut as tiny inclusions in dolomite.

Rutile forms small euhedral grains that outline skeletal shapes probably belonging to original detrital heavy minerals, in some cases overgrown by euhedral albite. Some tiny grains of rutile are included in vanadian chlorite and under quartz overgrowths, and are overgrown by supergene vanadate minerals. In the Norma Jean #2 mine dumps, one sample contains euhedral rutile or anatase grains growing off of quartz overgrowths.

Globules of what appear to be asphalt or bitumen (Fig. 4C, D, F, G) are present in several samples from the Schoolmarm decline (Bull Canyon), the Van #4 (Monogram Mesa), the Blue Streak mine (Bull Canyon), and the La Sal mine workings (La Sal district), notably in the high-grade ores. EPMA/EDS indicates that the main detectable element in the globules is C, with minor S. In contrast to the plant coal, globules of this material are structureless, lack cellular features, and decrepitate under the EPMA beam. These are found outside of quartz overgrowths, which are strongly corroded where they contact the black material (Fig. 4f). At the Blue Streak mine, though not in other Salt Wash ores, these globules are extremely abundant in a striped part of the ore zone known as "bacon rock" and are mixed with mostly framboidal, slightly arsenian pyrite (4–6 mass %

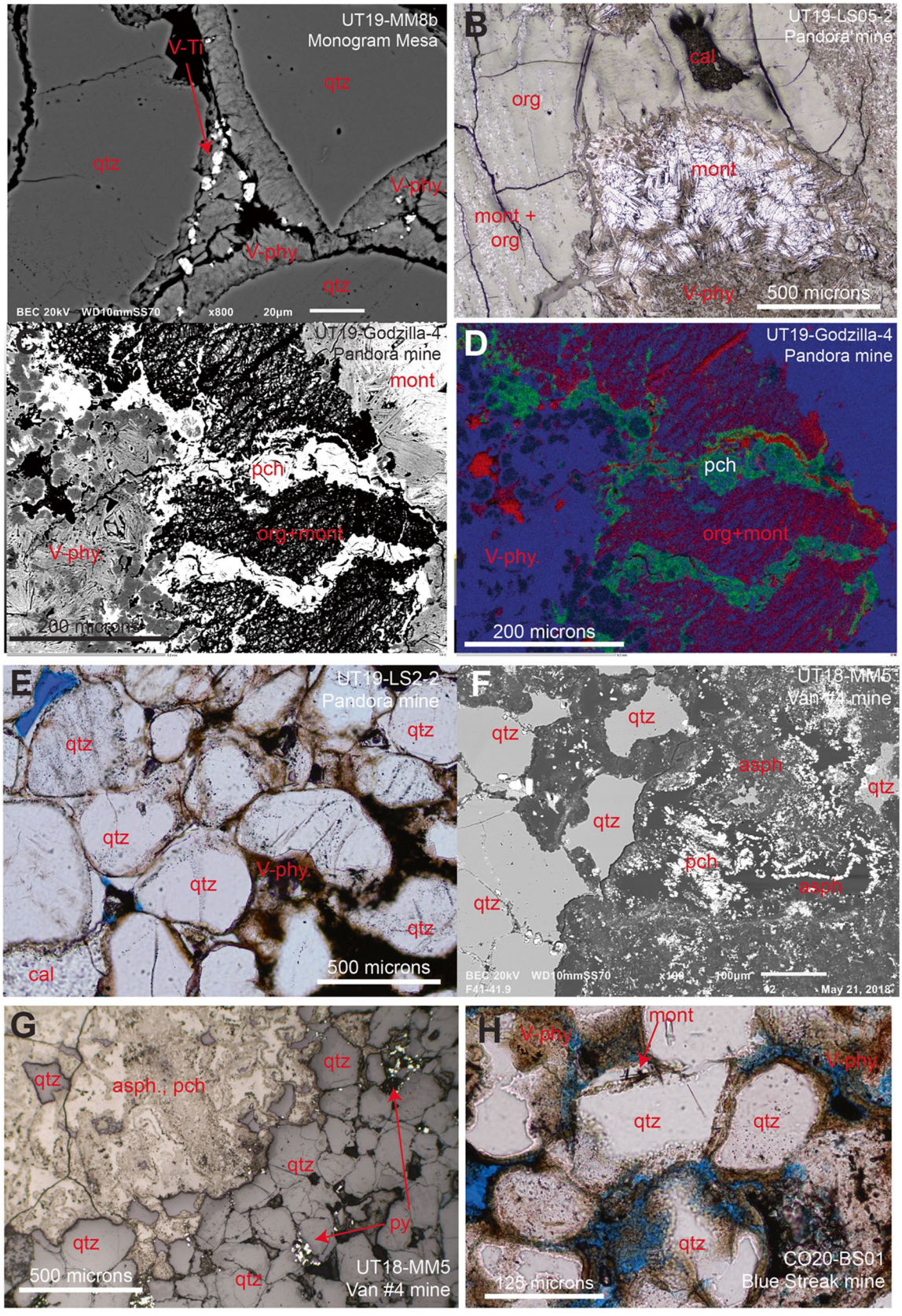
UT19-MM8b
Monogram Mesa
V-Ti
qtz
qtz
V-phy
V-phy
qtz
BEC 20kV WD10mmSS70 x800 20µm
B
UT19-LS05-2
Pandora mine
cal
org
mont
mont +
org
V-phy
500 microns
UT19-Godzilla-4
Pandora mine
mont
pch
org+mont
V-phy
200 microns
D
UT19-Godzilla-4
Pandora mine
pch
org+mont
V-phy
200 microns
E
UT19-LS2-2
Pandora mine
qtz
qtz
qtz
qtz
V-phy
qtz
qtz
cal
500 microns
F
UT18-MM5
Van #4 mine
qtz
qtz
qtz
asph
qtz
qtz
pch
asph
qtz
BEC 20kV WD10mmSS70 x100 100µm
F41-41.9 #2 May 21, 2018
G
qtz
qtz
asph., pch
qtz
qtz
py
qtz
500 microns
qtz
UT18-MM5
Van #4 mine
H
V-phy
mont
V-phy
qtz
qtz
qtz
125 microns
CO20-BS01
Blue Streak mine

◂**Fig. 4** Various minerals and textures in the Salt Wash U-V deposits. **A** V-phyllosilicate (V-phy) fringe around quartz (qtz) grains, enclosing inclusions of V-Ti oxide (V-Ti); compare (**E**) and (**H**). **B** Massive montroseite (mont) around and within organic matter (org) at the Pandora (La Sal) mine, surrounded by vanadian illite (V-phy) in transmitted ppl. Cal = calcite. **B** Montroseite (mont) amid a V-phyllosilicate matrix near a globule of organic (org) material. Fine, bright-white grains in left side of organic material are montroseite. Plane-polarized reflected light. **C** High-grade U-V ore at the Pandora-La Sal mine, consisting of a globule of organic matter impregnated with V oxides, veined by pitchblende (pch), and surrounded by montroseite and V-phyllosilicates in SEM photomicrograph. **D** Elemental RGB map of vanadium (blue), carbon (red), and uranium (green) distribution in (**C**). **E** Quartz overgrowths are present on the left side of the image but are increasingly replaced by brown V-phyllosilicates going right. Where intact, overgrowths enclose lines of mineral inclusions, dark. Plane-polarized transmitted light. Fsp = feldspar. **F** A mineralized asphalt (asph) globule at the Van #4 mine, Monogram Mesa in SEM photomicrograph. **G** Alternate view of the asphalt globule in (**F**), showing pyrite-rich (py) fringe and surrounding sandstone in reflected ppl. **H** Vanadium ore from the Blue Streak mine, Bull Canyon, Colorado, showing montroseite inclusions under quartz overgrowths and fringes of brown V-phyllosilicates replacing quartz overgrowths, transmitted ppl. Blue in **E** and **H** is epoxy

As by EDS). The dark bands do not themselves carry U-V mineralization, but the bacon rock occurs exclusively in the high-grade zone.

Two-phase fluid inclusions with large vapor bubbles were found under quartz overgrowths at La Sal and Blue Streak. The coarse cementing carbonate contains three-phase fluid inclusions with vapor bubbles and colorless daughter crystals at Blue Streak; in most of the other mines, the carbonate cement has two-phase, liquid–vapor inclusions only.

### 3.2.3 Metallic Mineralization

The major U mineral in the Salt Wash deposits is pitchblende, which forms inclusions under quartz overgrowths and within asphalt blobs, and at the Cougar group of mines was observed as inclusions in calcite. In extremely high-grade samples, ore minerals are found replacing detrital sandstone components [94]. The most common texture of all ore minerals, however, is interstitial space-filling (Fig. 4A, B).

Vanadium occurs as V (hydr)oxides and phyllosilicates. The V-hydroxides form clusters of small needles, some included under quartz overgrowths, some outside of quartz overgrowths and forming radiating fans amid the V-phyllosilicates (Fig. 4B, H; see also Bos Orent et al., this volume). The V-hydroxides were identified petrographically and by SEM as montroseite, but a powder XRD analysis of pulverized samples identified nolanite and fernandinite [95]. Compositions determined by EPMA corresponded mainly to montroseite for needles locked within or under quartz overgrowths, and to duttonite and other $V^{4+}$ minerals for those occurring outside the overgrowths [73, 95]. This is supported by TEM–EELS analyses, which found roughly $V^{4+}$ oxides as nanoscale crystals interleaved with, or at the edges of, V-illites [74]. The dominance of $V^{4+}$ minerals may not reflect the original hypogene mineralogy of the samples, as Evans [96] records that $V^{3+}$ is unstable in air and montroseite samples exposed to atmospheric conditions quickly oxidize to paramontroseite. All the V-hydroxides observed contain several wt% Fe, with no obvious compositional zoning or consistent geological patterns. At Blue Streak, the Fe content of the V-hydroxides commonly approaches 20 mass %.

An unknown U-V oxide is common in most unoxidized ore-bearing samples observed. These U-V oxide grains are of uncertain nature, but form irregular masses floating in the V-phyllosilicate matrix outside of quartz overgrowths. They are commonly intergrown with a Ti-V oxide, possibly tivanite, overgrow montroseite, and form inclusions in pyrite. In one sample from the Schoolmarm mine in Slick Rock, the U-V oxide occurs as interstitial needles resembling montroseite but containing more U than V.

A significant amount of the V in Salt Wash ores is hosted in phyllosilicates, which are common as an interstitial cement or matrix similar in texture and habit to the non-vanadian cementing clay. The V-phyllosilicates form soft radiating fans centered around quartz grains, contain inclusions of V-hydroxide, pyrite, clausthalite, and ferroselite, and in several instances clearly replace now-defunct quartz overgrowths. In samples with abundant V-phyllosilicates, no preserved quartz overgrowths remain and the remaining quartz grains are heavily embayed; replacement of claystone clasts is less common but is observed. Calcite overgrows the V-phyllosilicate. The V-phyllosilicates are typically light to medium brown in plane-polarized light and occur in two distinct compositions, a magnesian V-chlorite and a V-illite, at most of the Salt Wash deposits studied [73]. At Blue Streak, there are three types of V-phyllosilicates: the V-chlorite dominates along with a K-deficient V-biotite, while V-illite is rare. An earlier detailed study of the vanadian phyllosilicates showed that the vanadian illite and chlorite are in fact interlayered V-mica and a hybrid V-mica-montmorillonite with only a minor chlorite component [97], interleaved with paramontroseite [75, 76]. Quartz tends to be heavily corroded in mineralized areas carrying high concentrations of V-phyllosilicates, and sutured with a texture that Garrels et al. [76] termed microstylolites. The almost ubiquitous association of V-phyllosilicates with the extremely corroded quartz led Garrels et al. [76] to suggest that the V-clays had precipitated at the expense of the silica in the quartz. This interpretation is strongly supported by the textural and occurrence relationships documented in this work.

U-V mineralization in the Salt Wash is accompanied by a diverse suite of accessory metallic minerals. The most common sulfide is pyrite, which forms inclusions under

**Table 5** Mineral inclusions under quartz overgrowths in Paradox Basin U-V deposits

| Deposit type | Location | Overgrowth abundance | Inclusions under overgrowths | Comments |
|---|---|---|---|---|
| Salt Wash | Pandora/Beaver | Very common | Hematite, pitchblende, pyrite, U-V oxide, montroseite, monazite | Also contains hematite inclusions under feldspar overgrowths |
| | Legin group | Common | Hematite, rutile, barite | |
| | Charles T group | Common | Hematite, pitchblende, montroseite(?) | |
| | Norma Jean #2 | Common | Hematite | |
| | Cougar group | Common | Pitchblende | |
| | Van #4 | Common | Pitchblende, pyrite, montroseite | |
| | Unnamed rim cut | Common | Hematite, pitchblende, rutile, Ti-V oxide, apatite | Double overgrowths with inner hematite, outer pitchblende inclusions |
| | Schoolmarm | Common | Pitchblende, montroseite, U-V oxide | |
| | Blue Streak | Common | Hematite, pitchblende, montroseite | Also contain liquid–vapor fluid inclusions |
| Entrada-hosted | Omega Group | Common | Pitchblende, U-V oxide | |
| Chinle–Big Indian | Mi Vida | Rare | Hematite, pitchblende, barite | |
| | Serviceberry | Rare | Pitchblende | |
| | Homestake | Rare | Hematite | Double overgrowths present, both layers hematite |
| | Big Buck (Chinle) | Rare to moderately rare | Hematite, pitchblende, rutile, less commonly apatite and barite | Also contain liquid–vapor fluid inclusions |
| Chinle–San Rafael Swell | Temple Mountain | Common (Jw) to rare (TRc) | Hematite, pitchblende, rutile, less commonly celestine, monazite, sphalerite, niccolite(?) | Chinle overgrowths mostly turned to clay; in Wingate, liquid–crystal fluid inclusions |
| | Dirty Devil | Common | Hematite, pyrite, pitchblende(?) | Also contain liquid–vapor fluid inclusions |
| | Delta | Mod. common | Hematite, pitchblende, pyrite, rutile(?) | |
| | Lucky Strike | Rare | Pitchblende(?) | |
| Cutler-hosted stratigraphic | Big Buck (Cutler) | Mod. common | Hematite, pitchblende, V(-Ti) oxide, montroseite, apatite, rutile | |
| Cutler-hosted structural | Atomic King | Not observed | n/a | |

quartz overgrowths, small freestanding grains, multi-grain rosettes, or large interstitial masses (possibly nodules) amid the interstitial (V-)phyllosilicate cement. Framboidal pyrite, which is particularly common in coalified plant remains, is a small minority of the overall pyrite content of the rocks, except for the bacon rock at Blue Streak where framboids are extremely abundant and arsenian as noted above. Small cubic grains commonly fringe the asphalt globules, and occur within the asphalt mixed with pitchblende. The freestanding or interstitial pyrite overgrows montroseite, quartz, and quartz overgrowths, and barite. Embayment of the quartz overgrowths and barite at their contacts with the pyrite suggests that the pyrite may have partially replaced the quartz and the barite. The pyrite is overgrown by the V-phyllosilicates, clausthalite, chalcopyrite, and ferroselite. In some samples, it is also replaced by hematite and found overgrown by azurite; at the Cougar mines, pyrite forms tiny inclusions in cementing calcite. Silver minerals were observed only at the Cougar mines, with microscopic grains of argentite or acanthite forming inclusions in pyrite and in malachite and azurite.

Chalcopyrite is also common. It is a minor constituent of the inclusions under quartz overgrowths and is caught between quartz grains at microstylolites where they are sutured together. Larger grains of chalcopyrite overgrow pyrite, quartz and quartz overgrowths, and clausthalite, and are surrounded by V-phyllosilicates. In oxidized samples, it is partially to completely replaced by a mix of high-Cu

limonite, digenite, and covellite, which in some samples are surrounded or partially replaced by malachite and azurite.

Clausthalite and ferroselite are locally abundant in the La Sal mine complex, overgrowing pyrite as anhedral to subhedral interstitial grains and overgrown by galena and V-phyllosilicates. The clausthalite forms veinlets that crosscut the ferroselite. Among other occurrence types, both are found around the fringes of a dinosaur femur replaced by high-grade U-V ore. At Blue Streak, ferroselite was not observed but clausthalite is abundant, and apparently forms a solid solution with galena: both end-members occur along with a Pb(S,Se) species with a range of compositions. Brooks and Campbell [94] found a positive correlation between Pb and Se grades, which were especially enriched in the high-grade V ores, indicating that clausthalite represents a significant fraction of the Pb occurrence at La Sal. Another locally common mineral is sphalerite, which is found at the Van #4 mine on Monogram Mesa as coarse, Fe-poor anhedral grains in interstices, surrounding quartz overgrowths. Macroscopic, euhedral Fe-poor sphalerites with variable minor Cd occur at Blue Streak, along with microscopic freestanding grains overgrowing galena, pyrite, and quartz overgrowths. Sphalerite was not observed in other Salt Wash samples, though the rutile from the Schoolmarm mine has detectable Zn. In various samples, galena forms fine-grained fringes on pyrite, quartz overgrowths, V-chlorite pseudomorphing the quartz overgrowths, and clausthalite, and is surrounded by calcite and supergene minerals. Galena from the Schoolmarm mine contained several wt% Cu and Zn. Molybdenite was observed only at the Blue Streak mine as a sub-micron-sized grain within an asphalt globule, yielding a high-Mo SEM–EDS analysis; the identification is tentative.

Supergene minerals are numerous and varied. Texturally, they crosscut, overgrow, or surround all other minerals. Tyuyamunite and carnotite are both common, as are other metallic vanadates tentatively identified by SEM–EDS as tangeite, volborthite, veisgnieite, and lyonsite. All of the vanadates are overgrown by chrysocolla, azurite, and/or malachite where supergene Cu minerals are present, and commonly also by jarosite. A Cu-rich limonite, possibly goethite, is also common. The acanthite, where included in supergene Cu minerals, may also be supergene. In one sample, a dolomite forming coarse rhombs intergrown with malachite and azurite contains between 2 and 5 wt% Fe without detectable Mn.

## 3.3 Entrada Deposits

### 3.3.1 Detrital

As with the Salt Wash deposits, the chief detrital mineral in the Entrada-hosted deposits is quartz. In altered and mineralized samples, the edges of quartz grains are noticeably corroded. Quartzite, carbonate, siltstone, and mudstone lithics are also common, with rare feldspar grains as well. Detrital zircon is present in trace abundances. Minor detrital Ti oxide (1–2%) is present, with the textures of some grains and consistent trace concentrations of V, Fe, Mn, and Ca indicating conversion from original ilmenite-magnetite. No fossils or plant coal were noted. Grain sizes are highly variable: most of the sandstone is fine- to medium-fine-grained, but a minority of grains are coarse to very coarse and sorting is minimal. Except in high-grade samples, porosity is estimated visually at 10–15%, with minor clay occlusion.

### 3.3.2 Alteration

Alteration type correlates with macroscopic color and ore grade. In weakly mineralized rocks, usually purple or colorless, detrital quartz cores are surrounded by authigenic overgrowths of quartz. Most of these are hexagonal and euhedral, but in a few places the overgrowths still showed a chalcedonic birefringence indicating incomplete ripening into quartz. These overgrowths enclose lines of < 5-micron inclusions identified as hematite in non-ore samples and as V-bearing pitchblende in ore zones (Table 5, Fig. 5C, D, H). Sutures between quartz grains are common and crosscut the overgrowths. In mineralized areas, which are green, overgrowths are absent, with trace remnants indicating they probably once existed but have been corroded away (Fig. 5F).

Barite is a very common accessory phase and helps cement the rock in and near ore zones. It most commonly forms fine lath-shaped euhedral crystals in interstices, sometimes with nucleation points on the edges of quartz overgrowths. Strontium is detectable in nearly all crystals measured but is usually < 1.5 atom%. Barite is common at < 5% abundances in most of the thin sections, but is particularly abundant near crosscutting veins of sparry calcite. Other minor but present alteration minerals include normally detrital minerals such as apatite and rutile. Apatite is found as fluorapatite forming small, highly euhedral hexagonal grains in interstices, with no discernible textural relations to other alteration minerals or internal zoning. Rutile forms tiny clusters of euhedral crystals growing off quartz overgrowths into pore space.

Clays are interstitial and in some samples help cement the rock. In ore zones, nearly all sheet silicates present are end-member roscoelite, but in unmineralized samples the compositions are illite to illite-dominated mixed-layer clays, consistent with the findings of Breit [45]. As with their vanadian equivalents, the normal clays encircle quartz grains,in areas with abundant clay, the quartz overgrowths are either absent or strongly corroded. There was no clear textural relationship between vanadian and non-vanadian phyllosilicates, which generally were not found in the same samples. Needles or

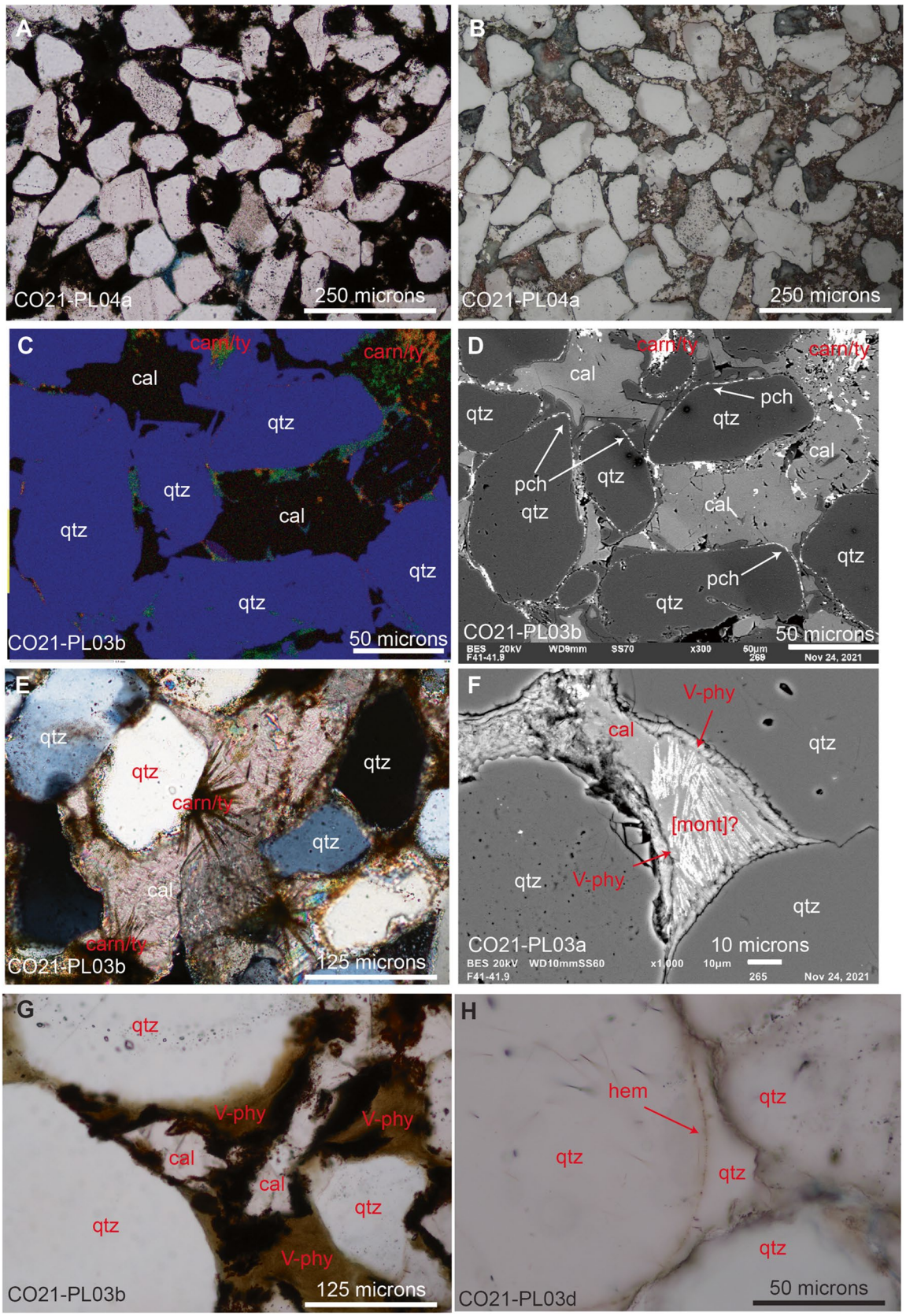
A
CO21-PL04a
250 microns
B
CO21-PL04a
250 microns
C
carn/ty
carn/ty
cal
qtz
qtz
qtz
cal
qtz
qtz
CO21-PL03b
50 microns
D
carn/ty
carn/ty
cal
pch
qtz
qtz
pch
qtz
qtz
cal
cal
qtz
pch
qtz
CO21-PL03b
50 microns
BES 20kV WD9mm SS70 x300 50µm 269 Nov 24, 2021
F41-41.9
E
qtz
qtz
qtz
carn/ty
qtz
cal
carn/ty
CO21-PL03b
125 microns
F
V-phy
cal
qtz
[mont]?
qtz
V-phy
qtz
CO21-PL03a
10 microns
BES 20kV WD10mmSS60 x1,000 10µm 265 Nov 24, 2021
F41-41.9
G
qtz
V-phy
V-phy
cal
cal
qtz
qtz
V-phy
CO21-PL03b
125 microns
H
hem
qtz
qtz
qtz
qtz
CO21-PL03d
50 microns

◂**Fig. 5** Minerals and textures in the Entrada (U-)V deposits near Placerville, CO. **A** Fine to medium-fine quartz sandstone host rock, featuring interstitial iron oxides and dark, opaque globules mentioned in the text, transmitted ppl. **B** Reflected-light view of (**A**). **C** SEM–EDS map of ore sample showing vanadian pitchblende necklaces under quartz overgrowths and partial replacement of overgrowths by roscoelite fringe. Supergene carnotite and tyuyaminute (carn/ty) are present in the calcite cement. Red = U, green = V, blue = Si. **D** Backscattered electron photomicrograph of (C). Cementing interstitial crystals are calcite. **E** Calcite cementing quartz grains with U-vanadate staining and urchin-shaped carnotite-tyuyamunite sprays, transmitted xpl. **F** Possible pseudomorphed montroseite, now Fe oxide, in between detrital quartz grains fringed by roscoelite; compare Fig. 4A. Backscattered electron photomicrograph. **G** Common texture of roscoelite (brown), found fringing quartz grains and as interstitial cement, conoscopic transmitted ppl. **H** Hematite (hem) inclusions under quartz overgrowth, conoscopic transmitted ppl

lines of Ti oxide, with textures suggesting exsolution, are common features in the V-phyllosilicate cement. Some clay forms inclusions in the barite and a carbonate, which is the principal cement for most of the rocks outside the high-grade zone. The carbonate is a coarse, sparry calcite containing liquid–vapor fluid inclusions, which engulfs all other mineral phases except the supergene vanadates and interstitial hematite. In a few samples, it forms veins of coarse crystals overgrowing barite laths. Although mostly stoichiometric calcite with no detectable Mn or Fe, the Mg content varied unsystematically up to 1.5% Mg by EDS.

Interstices between quartz grains were also found to contain globules of a dark brown to black, opaque material and a colorless, transparent material, both isotropic and probably amorphous. Both were structureless and displayed low reflectivity and low relief. Examination by SEM indicated that both have a carbonaceous composition; they may be hydrocarbon remnants but the lack of distinctive features precludes definitive identification.

#### 3.3.3 Metallic Mineralization

The main ore mineral in the Entrada deposits is roscoelite (Table 3) forming fringes around detrital quartz cores, with textures indicating that the roscoelite replaces quartz overgrowths (Fig. 5G). Its textural relationships with other authigenic minerals are the same as those of the non-vanadian clays. In high-grade zones, the roscoelite is the main cement to the rock; Breit [45] documented rocks consisting of up to 70% roscoelite. New EDS, EPMA, and TEM analyses shows that the compositions are not K-deficient and consistently contain 7–9 atom% V, close to end-member roscoelite [98]. This contrasts with the other deposit types in the Paradox Basin, where V-phyllosilicate compositions vary from V-illite to V-chlorite even within individual samples, true roscoelite is rare, and V content covers a wide range. From vanadian and non-vanadian illites in the Entrada-hosted deposits around Placerville, Breit [45] obtained Rb–Sr ages in the mid-Tertiary.

Montroseite is notable for its absence from the rock, even in the highest-grade samples. Prismatic crystals of a mildly vanadiferous iron oxide in interstices of the high-grade zone may represent pseudomorphs of Fe-rich montroseite, but are extremely rare and not definitive. Mariposite or Cr-mica, reported from the lower fringes of Entrada-hosted V deposits, was not observed [45, 79].

Pitchblende occurs only as micron-scale inclusions under quartz overgrowths (Fig. 5C, D). These necklaces are common on the fringes of high-grade V zones, where quartz overgrowths have been preserved. Uniformly, the pitchblende contains V as well as U. The only other accessory hypogene mineral found is pyrite, which forms tiny cubes in the interstices between quartz overgrowths and is mainly oxidized to hematite. Fischer [40] and Spirakis [79] reported galena and clausthalite in Entrada-hosted deposits, but none was observed in the limited number of samples examined in this study.

All samples displayed a strong supergene overprint. Hematite is common, in a few cases replacing pyrite and possibly montroseite, but more often as poorly crystalline intergranular masses with globular morphology and red internal reflections. More abundant still is Ca-dominated tyuyamunite-carnotite, which forms sea urchin-shaped clusters fringing carbonate, barite, and quartz grains and has a characteristic green–brown color in thin section. Minor amounts of base-metal vanadates, including probable rossite and hewettite or metahewettite, were also observed. All vanadates and hematite overgrow the other minerals in the thin sections.

### 3.4 Chinle-Hosted Deposits

#### 3.4.1 Detrital

The major detrital components of these arkosic sandstones are quartz, feldspar, micas, and micrite and claystone clasts. Feldspars include both tartan and plagioclase types of twinning, but all measured and reported compositions are heavily potassic with only minor albite and no detectable anorthitic component. Textural evidence indicates that at least at Big Buck, some of the albite is an authigenic replacement of K-feldspar, but this was observed in only one sample. Detrital muscovite is common and slightly phengitic with minor Fe. Detrital biotite is rarer but present, and is incompletely altered with tiny crystals of exsolved rutile along cleavages. One sample from Big Buck also showed pitchblende invading biotite along cleavage planes. Microprobe analysis of Big Indian samples revealed a substantial V content in detrital micas of both types.

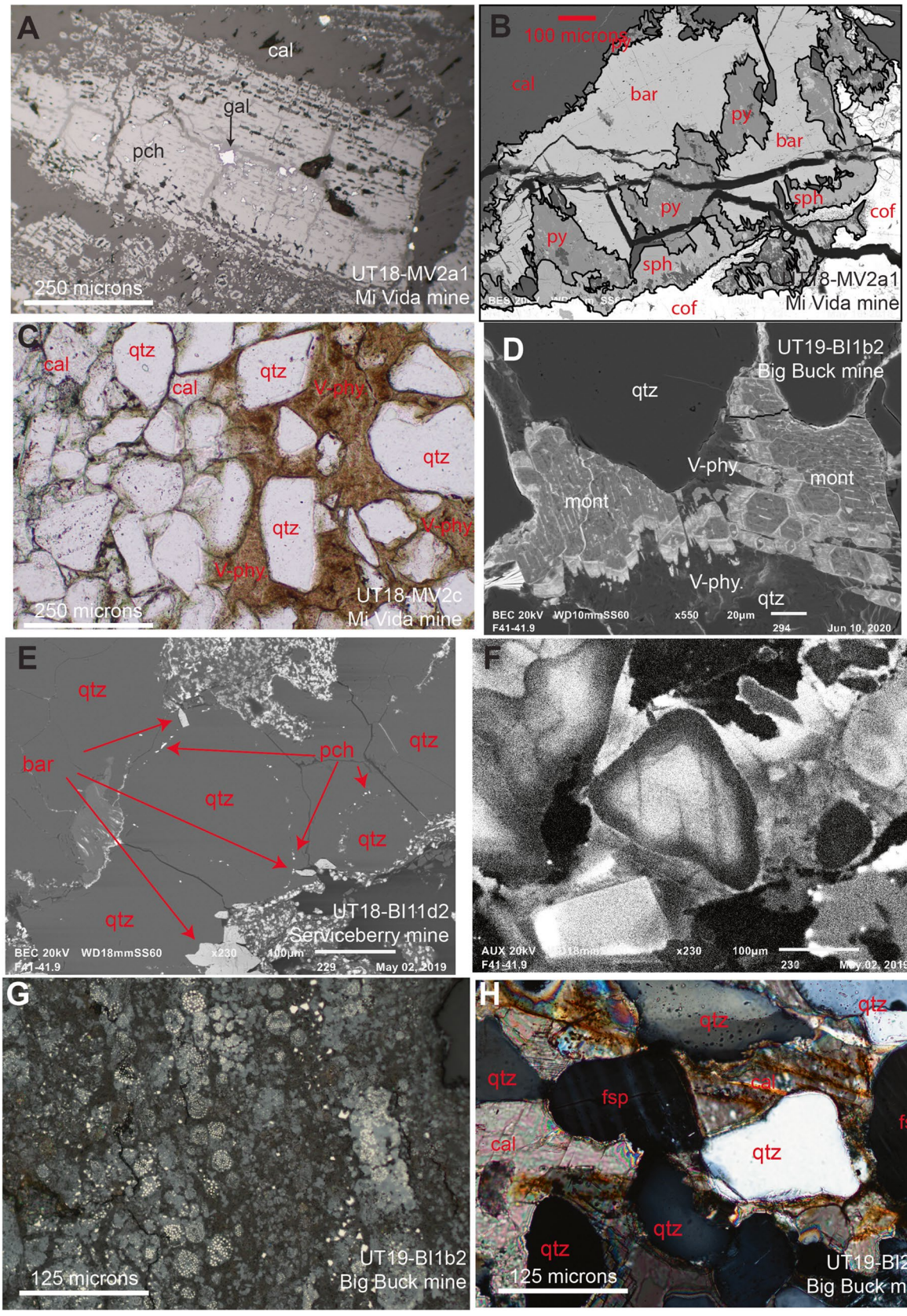
A
cal
gal
pch
250 microns
UT18-MV2a1
Mi Vida mine
B
100 microns
cal
bar
py
bar
py
sph
cof
py
sph
cof
8-MV2a1
Mi Vida mine
C
cal
qtz
cal
qtz
V-phy.
qtz
qtz
V-phy.
V-phy.
250 microns
UT18-MV2c
Mi Vida mine
D
UT19-BI1b2
Big Buck mine
qtz
V-phy.
mont
mont
V-phy.
qtz
BEC 20kV WD10mmSS60 x550 20µm
F41-41.9 294 Jun 10, 2020
E
qtz
qtz
bar
pch
qtz
qtz
qtz
UT18-BI11d2
Serviceberry mine
BEC 20kV WD18mmSS60 x230 100µm
F41-41.9 229 May 02, 2019
F
AUX 20kV x230 100µm
F41-41.9 230 May 02, 2019
G
125 microns
UT19-BI1b2
Big Buck mine
H
qtz
qtz
qtz
qtz
fsp
cal
fsp
cal
qtz
qtz
qtz
125 microns
UT19-BI2b2
Big Buck mine

◂**Fig. 6** Minerals and textures in the Chinle Big Indian U-V deposits. **A** Pitchblende replacing cellular organic material, probably plant coal, with galena occupying veins in the middle, at the Mi Vida mine. Surrounding gray material is calcite. Reflected ppl. **B** Complex texture from Mi Vida ore, showing coffinite overgrown by Cd-rich and Fe-poor sphalerite and pyrite. The pyrite also grows around the barite. SEM photomicrograph with contacts traced for greater clarity. **C** Sharp boundary between calcite cement and V-phyllosilicate cement at Mi Vida; note that much of the interstitial texture present in the calcite-cemented zone is destroyed where V-phyllosilicates cement the rock. Compare Figs. 4a and 5g. Transmitted ppl. **D** Montroseite cementing detrital quartz in high-grade ore at the Big Buck mine. The prominent zoning in crystals reflects variable U content (see text for discussion). SEM photomicrograph. **E** Quartz overgrowths at the Serviceberry mine encapsulate pitchblende inclusions and are pierced by barite crystals. Note ragged boundary of quartz grains at contact with mixed pitchblende-V-phyllosilicate cement. SEM photomicrograph. **F** The same sample view as in (**E**), shown in blue-band cathodoluminescence. Detrital quartz cores and authigenic overgrowths around inclusions are clearly visible. **G** Pitchblende cementing framboidal pyrite in high-grade ore sandstone at the Big Buck mine. Euhedral pyrite is visible outside the pitchblende-pyrite cementations. Reflected ppl. **H** Post-ore carbonate cement at the Big Buck with streaks of brown-orange fluid inclusions. Transmitted xpl

Micrite and claystone clasts are well-rounded and up to 2–3 cm. Plant remains, identified by their cellular structures, are uncommon among the clasts in the channel conglomerates and sandstones, but are abundant in the intercalated shales in the Big Buck mines; plant remains are rarer at other Big Indian mines according to contemporaneous reports [58]. Analyses by Kennedy [59] suggest that the average ore from Big Indian mines contained < 0.35% organic C, and generally < 0.2%, without variation between mineralized and barren rocks. No correlation is known between U-V mineralization and plant coal or other forms of organic C [57]. This is also the case in the White Canyon deposits, where wood fragments are well known but only about 40–50% are mineralized with pitchblende and chalcopyrite [47, 50]. Heavy minerals are noticeably scarce in the Chinle deposits. So far as can be determined, the only detrital heavy minerals are zircon and what used to be ilmenite, now altered to hematite and rutile.

### 3.4.2 Alteration

A notable feature of the Chinle-hosted deposits is quartz overgrowths, though rarer than in their Salt Wash counterparts. Rarely, quartz clasts exhibit thin overgrowths of less well-crystallized silica forming euhedral hexagons. The overgrowths' authigenic nature is indicated by their well-developed hexagonal angles and by CL images, which invariably show that the overgrowths are much less luminescent than the detrital cores and are commonly sector-zoned. Quartz overgrowths are rare and generally thin, but have been observed on the SEM in samples from all deposits of this type visited; they are also attested in the literature [47, 50]. The overgrowths enclose lines of mineral inclusions that dust the rims of the detrital cores and are about 1–3 microns across. EDS analyses show that these are mostly hematite or pitchblende, more rarely apatite, barite, or rutile (Table 5. Fluid inclusions are also present beneath these overgrowths, mostly too small to permit detailed observation; the few that were large enough to observe were two-phase liquid-dominated inclusions with small vapor bubbles. Most of the fluid inclusions observed below quartz overgrowths are colorless, but a minority has a definite orange tint. Overgrowths were not observed around feldspar grains, and those around quartz are commonly crosscut by sutures that weld quartz grains together—a feature also observed by Gross [83]. Trains of secondary fluid inclusions in the quartz grains show strong blue fluorescence under ultraviolet microscopy.

The textures and occurrence patterns of a relatively common feature, fringes of clay around the detrital quartz grains, suggest that quartz overgrowths were once much more abundant but that many of them were cannibalized during clay formation. While most of these clays have illitic compositions with minor Mg and Fe peaks on EDS, they are also commonly vanadian (discussed below). Apart from fringing quartz grains, the (V-)clays also occur as interstitial fillings around pyrite, montroseite, and detrital grains. (Fig. 6C) Non-vanadian clays are also reported at Big Indian as kaolinitic and as mixed-layer illite-montmorillonite by Jacobs [69], with dickite developing near fault zones. Kaolinite is commonly reported in bleached quartzarenites such as the Wingate Formation, particularly associated with quartz overgrowths [99].

The alteration phases also include minerals that are more commonly detrital. Rutile occurs as clusters of small, disseminated euhedral grains, likely authigenic, in interstices, fringing quartz overgrowths and within masses of (V-)clays. Monazite also forms euhedral grains in interstices; Mi Vida monazite was found containing inclusions of pitchblende or coffinite. Rare fluorapatite, observed at Mi Vida under quartz overgrowths, contained inclusions of galena and vanadian phyllosilicate. Apatite at Big Buck forms small euhedral crystals nestled amid the (V-)clays, F-dominated but with detectable Cl; larger apatites contain pyrite inclusions. Barite is a minor phase. In addition to its rare occurrences under the quartz overgrowths, barite forms interstitial laths with variable Sr contents, up to 7 atom% by EDS. In the high-grade samples from Mi Vida, two types of barite were observed. One has a ratty texture and overgrows plant matter that has been replaced by pitchblende; this barite is partially replaced by pyrite. The second barite is coarser and pristine and overgrows pyrite, sphalerite, U-V minerals, and in places also overgrows the cementing calcite. Celestine was detected at Big Buck as large, Ba-poor interstitial masses found surrounding quartz grains and quartz-fringing clays, but was not found in other Chinle-hosted deposits of

this type. However, Schmitt [58] reported widespread barite and celestine as veins in close proximity to the Lisbon Valley fault and its subsidiaries at the northwest and southeastern ends of the anticline. He suggested that celestine dominates the sulfate suites at the northern end of the anticline and grades southward to Ba-dominant compositions.

Carbonate is the most common cement for the Chinle rocks, occurring in both mineralized and unmineralized areas. The dominant composition is calcite, relatively pure with variable minor Mn (up to 0.3 mass %). Where both are present, the calcite overgrows the (V-)clays, the detrital minerals, and all non-supergene ore minerals. It contains inclusions of pyrite and of one type of barite. Fluid inclusions within the carbonate are very small but were observed to be two-phase, mostly liquid but with visibly mobile vapor bubbles. In contrast to previous observations [56], the coarse cementing calcite observed in this study was all found overgrowing hypogene ore minerals, not being replaced by them. Documenting calcite both replacing and replaced by ore minerals, Weir and Puffett [57] suggested multiple episodes of calcite deposition, dissolution, and reprecipitation. Calcite colored pink by microscopic hematite inclusions has been widely reported [57, 58, 83], but was not observed in this study.

Fluid inclusions occur underneath quartz overgrowths. Most are too small for detailed description, but at the Big Buck mine several larger examples were found to consist of two-phase liquid–vapor inclusions. At the Mi Vida mine, trains of secondary fluid inclusions in quartz fluoresced bright blue under ultraviolet light. The coarse cementing calcite in the Big Buck mine also contains two-phase liquid–vapor fluid inclusions.

#### 3.4.3 Metallic Mineralization

Pitchblende, a mix of uraninite and coffinite, is the dominant hypogene U mineral. Grains of pitchblende occur within quartz overgrowths, rarely, and also fringe detrital clasts and fill fractures within them. Pitchblende also replaces some of the plant coal, with coffinite filling cell centers and uraninite pseudomorphing the cell walls. However, the relationship between plant coal and pitchblende is inconsistent: plant coal may be heavily U-mineralized or completely devoid of detectable U. Multiple pockets of high-grade pitchblende were observed in one sample in which nearby plant coal was totally unmineralized. Schmitt [58] reported pitchblende penetrating feldspars and micas along cleavage plans, with partial to near-total replacement of the silicate grains,similarly, Gross [83] described ore minerals apparently corroding quartz grains and invading micas and feldspars as well at Mi Vida, and Trites and Chew [47] described the same texture at Happy Jack. Colloform textures have been reported in Big Indian district pitchblendes [58] but were not observed in this study. Pore-filling or cementing textures are common.

Vanadium is not reported from deposits around White Canyon but is abundant throughout the Big Indian district, to which alone the following descriptions relate. Montroseite or a related V-oxyhydroxide is the most common hypogene V ore mineral, occurring as radiating fans of prismatic crystals. These sit on the perimeters of detrital grains below (V-)clay fringes and in interstices between quartz grains, but were not observed underneath quartz overgrowths in any sample. Montroseite overgrows pitchblende and is overgrown by pyrite, V-phyllosilicates, supergene ore minerals, and by an unidentified U-V oxide. At both Mi Vida and Big Buck, montroseite compositions appear to cover most of the range from VOOH to FeOOH. Extremely U-rich compositions (up to 58 mass % U by EDS) were also noted at Big Buck, with strong chemical zonation and no apparent relationship to Fe substitution (Fig. 6D). However, crystal-chemical considerations suggest that this may have been duttonite or another tetravalent V oxyhydroxide, more likely than true montroseite to be able to accommodate $U^{4+}$. This would be compatible with the widely reported, unidentified "$V^{4+}$ oxide" described in Chinle-hosted Big Indian deposits in close association with the montroseite [83].

More abundant than montroseite at Big Indian are vanadian phyllosilicates, found in samples from all four mines and represent a major component of the cement in mineralized zones. These range from roscoelite (rare) to dominant V-chlorite and V-biotite. The V-biotite is K-deficient and, along with the V-chlorite, is heavily Mg-dominated. Identifiable by a distinctive brown color in plane-polarized light, antitaxial plates of V-phyllosilicate fringe quartz grains, montroseite, and pitchblende. In especially high-grade samples, V-phyllosilicates also partially replace some of the claystone clasts in the rock. Larger interstitial masses of the V-biotite and V-chlorite help to cement the clasts; this cementing form is overgrown by calcite. There is no observed consistent relationship between the occurrences of montroseite and V-phyllosilicate or between the different types of V-phyllosilicate, with all three sometimes occurring in the same sample. There is, however, a consistent tendency for quartz grain edges to be most heavily corroded in contact with the V-phyllosilicates, a tendency Schmitt [58] also observed in feldspar grains within high-grade V ore zones. As in other deposit types, this texture may reflect the cannibalization of quartz overgrowths and/or detrital quartz by alteration to V-phyllosilicates. Based on backscatter coefficient, the V-phyllosilicates are relatively homogeneous in composition.

Base metal sulfides are common accessory minerals in both White Canyon sandstone-hosted and Big Indian Chinle unconformity deposits. Pyrite is the most abundant, forming interstitial freestanding subhedral to euhedral grains.

Where quartz overgrowths occur, these pyrite grains sit outside of them. A minority in Big Buck, Homestake, and Mi Vida samples is framboidal, and at Big Buck a block of pyrite framboids was observed cemented by pitchblende and galena. Framboids have been previously observed in multiple now-inaccessible Big Indian district mines as well [58]. At Big Buck and Mi Vida, pyrite was found as large nodules engulfing detrital and some secondary minerals (pitchblende, sphalerite, and barite). The quartz thus surrounded has extremely ragged edges at contact with pyrite. At Mi Vida, pyrite also occurs as inclusions in coffinite, and is found intergrown with a high-Cd sphalerite. At Big Buck, pyrite is overgrown by galena, chalcopyrite, and the unidentified U-V oxide. Marcasite is also reported from multiple Big Indian Chinle mines but was not observed in this study [57]. Coleman and Delevaux [84] noted that the pyrite and associated sulfides from Chinle-hosted deposits contains < 0.01% Se, very low compared to the Se content in other sulfides and U deposits.

Sphalerite is found at Mi Vida with a high Cd content and no detectable Fe, likely corresponding to what Gross [83] and Schmitt [58] identified as greenockite. Textural relationships of the Mi Vida sphalerite indicate a similar paragenetic position to the euhedral pyrite, and the compositions of both sulfides support equilibrium co-precipitation of the pyrite and sphalerite [100]. Happy Jack reportedly contains accessory galena associated with pitchblende replacing plant coal, and sphalerite with plant coal not replaced by pitchblende [47].

Chalcopyrite is less abundant at Big Indian but still a common minor constituent of U-rich rocks, in many instances found as inclusions within digenite and covellite that probably replace it. At Happy Jack, chalcopyrite is the dominant base metal mineral and is common found in close association with pitchblende, typically replacing the interiors of cells whose walls have converted to pitchblende [47, 50]. Chalcocite and native copper were reported by Weir and Puffett [57] at Big Indian, the latter in mudstones near the orebodies, but were not observed in this study. These and un-replaced chalcopyrite grains are typically in the form of interstitial masses that overgrow pyrite and surround quartz overgrowths. Smaller grains form inclusions in clay cements. At Happy Jack, covellite and chalcocite are common and bornite occurs in exsolution textures with some of the chalcopyrite [50]. At Mi Vida, chalcopyrite grains overgrow the pyrite-sphalerite fringe on high-grade pitchblende ore. Galena is uncommon in Big Indian but forms inclusions in calcite and vanadian phyllosilicates, overgrows the montroseite fringes around quartz grains, cements pyrite framboids, and is found in close association with coffinite. The only other accessory sulfide identified in Big Indian deposits was molybdenite, one grain of which was found as an inclusion in a vanadian phlogopite at Big Buck in close association with galena. Molybdenite and jordisite have been widely reported from claystone layers in ore zones before, but few examples were observed in our samples. They may be similar to the "ilsemannite" that Miller [50] reported at White Canyon. Gersdorffite is reported at Happy Jack but was not observed in this study.

Multiple previous authors have remarked that supergene minerals are far less well-developed in Chinle-hosted unconformity deposits at Big Indian than in either Salt Wash- or Cutler-hosted deposits nearby. This is consistent with the results of this study. At Mi Vida, the only supergene mineral reported is metatyuyamunite [83]. Melanovanadite, carnotite, and tyuyamunite are reported from unspecified Chinle-hosted unconformity deposits as well [66]. In this study, minor amounts of malachite and carnotite were observed in thin sections, but the principal supergene mineral is tyuyamunite or metatyuyamunite with a distinct chartreuse color. Carnotite cements rosettes and masses of small tabular jarosite grains at Big Buck; whether this jarosite is part of the supergene mineralogy is not certain. Melanovanadite was not observed. In no case did supergene U and V minerals make up more than a very small proportion of the mineralization. Supergene development is somewhat greater in the Chinle sandstone-hosted deposits at White Canyon, with the list of oxidized minerals including uranopilite, schoepite, and zippeite among the U phases and malachite, azurite, brochantite, and antlerite as the supergene products of Cu [50]. Supergene oxidation of the minor constituents also forms jarosite, goethite, and erythrite [50].

## 3.5 Chinle San Rafael Swell Deposits

### 3.5.1 Detrital

Quartz is the main detrital component of the Chinle sandstones that host the ore, but feldspar and muscovite are also common. Although most of the feldspar displays plagioclase twinning, SEM–EDS shows mainly potassic compositions with minor Na if any. The majority of the muscovite observed in heavily altered zones and in ore deposits was partially broken down to a mixed-layer clay. Surviving muscovite showed a slightly phengitic composition with detectable Fe and Mg, a composition reflected in the replacing clays. Biotite is extremely rare and shows a strong development of rutile along cleavage planes, and its breakdown may have preceded the decomposition of the muscovite. Zircon and chromite are rare detrital minerals, and micritic and chalcedony clasts are a common component of the more conglomeratic host rocks. Detrital heavy minerals, other than zircon, are noticeably scarce, but small clusters of rutile suggest the replacement of detrital ilmenite or titanomagnetite. Fluorapatite was observed at Temple Mountain, but it is not clear whether the grains are clastic.

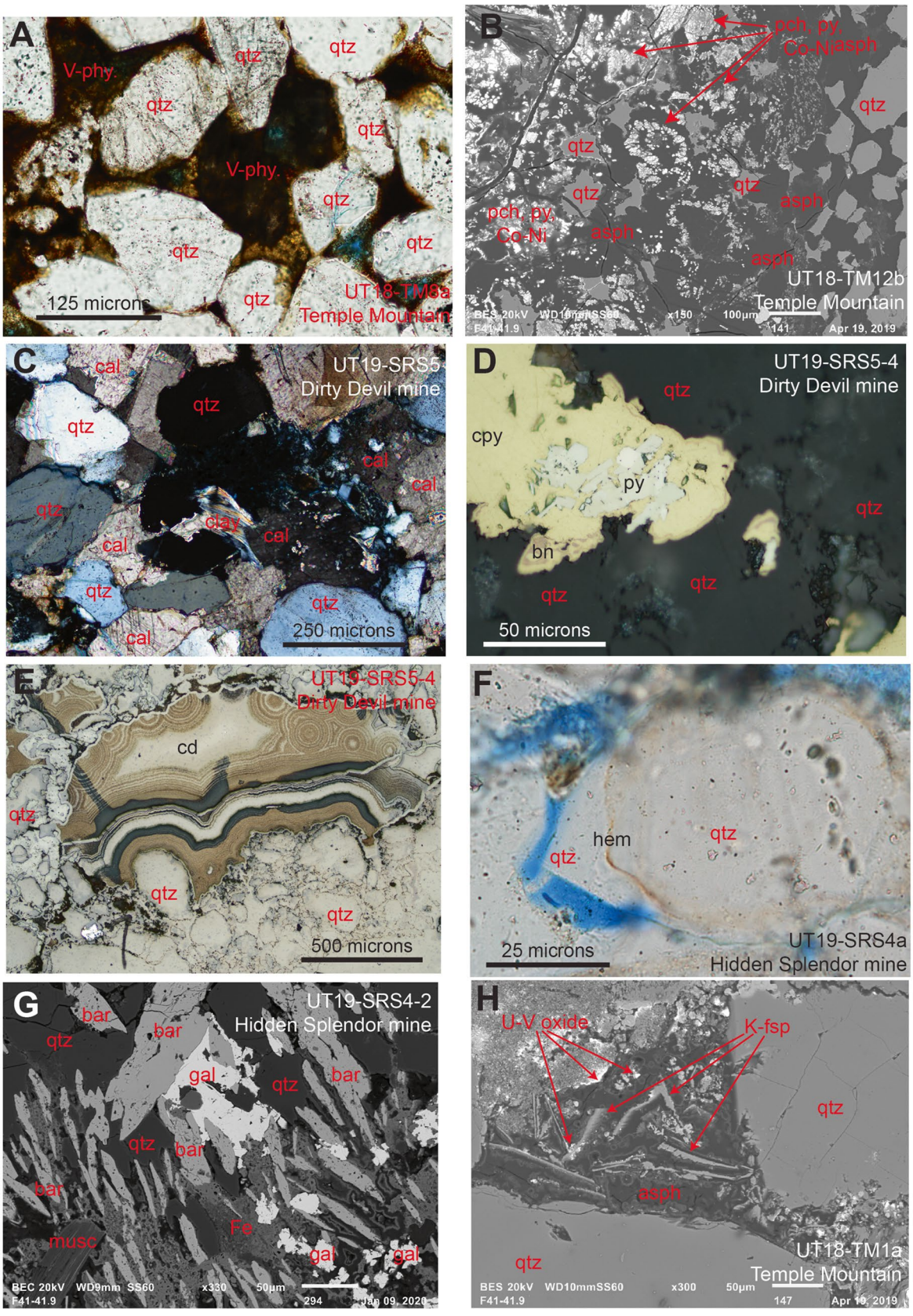
A
V-phy.
qtz
qtz
qtz
qtz
V-phy.
qtz
qtz
qtz
qtz
qtz
125 microns
UT18-TM8a
Temple Mountain
B
pch. py.
Co-Ni
asph
qtz
qtz
qtz
qtz
asph
pch. py.
Co-Ni
asph
asph
UT18-TM12b
Temple Mountain
BES 20kV WD10mmSS60 x150 100µm
F41-41.9 141 Apr 19, 2019
C
cal
qtz
qtz
UT19-SRS5
Dirty Devil mine
cal
cal
qtz
clay
cal
cal
qtz
qtz
cal
250 microns
D
qtz
UT19-SRS5-4
Dirty Devil mine
cpy
py
qtz
bn
qtz
qtz
50 microns
E
UT19-SRS5-4
Dirty Devil mine
cd
qtz
qtz
qtz
500 microns
F
hem
qtz
qtz
25 microns
UT19-SRS4a
Hidden Splendor mine
G
bar
bar
qtz
UT19-SRS4-2
Hidden Splendor mine
gal
qtz
bar
qtz
bar
bar
musc
Fe
gal
gal
BEC 20kV WD9mm SS60 x330 50µm
F41-41.9 294 Jan 09, 2020
H
U-V oxide
K-fsp
qtz
asph
qtz
UT18-TM1a
Temple Mountain
BES 20kV WD10mmSS60 x300 50µm
F41-41.9 147 Apr 19, 2019

◂**Fig. 7** Minerals and textures in the Chinle San Rafael Swell deposits. **A** Sandstone at Temple Mountain cemented by V-phyllosilicates (brown). Transmitted ppl. **B** Asphalt globule containing remnant quartz, pitchblende, pyrite, and a Co–Ni sulfide (Co–Ni) at Temple Mountain. SEM photomicrograph. **C** Calcite-cemented sandstone at the Dirty Devil mine, San Rafael Swell. Transmitted xpl. **D** Accessory metallic mineralization at the Dirty Devil mine, San Rafael Swell. Chalcopyrite, with intergrown bornite near crystal edges, contains inclusions of ferroselite and sphalerite. Reflected ppl. **E** Petroleum-stained chalcedony (cd) cementing Chinle sandstone at the Dirty Devil mine. Reflected ppl. **F** Hematite inclusions under quartz overgrowth, Chinle Formation, Hidden Splendor (Delta) mine. Transmitted ppl. **G** Edge of a partially oxidized pyrite nodule at the Hidden Splendor mine, with pyrite now converted to a Co- and Mn-bearing iron oxide (Fe) and galena (gal) overgrowing barite. SEM photomicrograph. **H** Authigenic K-feldspar and U-V oxide growing in an interstitial asphalt globule near quartz and K-feldspar (K-fsp) grains at Temple Mountain. Zoning in asphalt is caused by variations in trace Fe content. SEM photomicrograph

#### 3.5.2 Alteration

Overgrowths are well-developed around quartz grains in samples from the Temple Mountain, Lucky Strike, Dirty Devil, and Delta mines (Fig. 7F). The overgrowths are euhedral, but corroded where in contact with cementing clay, V-phyllosilicates, asphalt, or metal sulfides. Between overgrowth and detrital core are included tiny grains of hematite, pyrite, rutile, pitchblende, and liquid–vapor fluid inclusions; at Temple Mountain celestine, sphalerite, monazite, and a nickel arsenide are also among the inclusions found below quartz overgrowths. Sutures between quartz grains crosscut these overgrowths. Overgrowths were also observed around a small minority of feldspar grains, but these are poorly developed. In one sample from the Dirty Devil deposit, authigenic K-feldspar was found overgrowing quartz overgrowths, and at Temple Mountain, authigenic K-feldspar was observed within a blob of asphalt.

The dominant cements are carbonate and clays. Of carbonates, there are several types apart from the micritic clasts. A coarse-grained, variably Mn- and Fe-bearing dolomite cement contains pyrite and chalcopyrite grains, asphalt blebs, and two-phase liquid–vapor fluid inclusions, a few of which also have daughter crystals. The daughter crystals observed in the dolomite at the Delta mine are transparent, whereas those at Temple Mountain were dark and opaque. The dolomite overgrows mixed-layer clays and quartz and K-feldspar overgrowths, and is cross-cut by a dark, inclusion-rich carbonate with hematite along growth zones. Under the microscope, the coarse dolomite has slightly undulose extinction, and under SEM it shows a pronounced compositional zoning from Mn > Fe to Fe > Mn, with several % Fe in the more ankeritic zones. The clay, overgrown by the carbonate, occurs in inverse proportion to the amount of mica in the rock and has a distinct greenish tinge in plane-polarized light. SEM–EDS analysis shows a kaolinitic composition with variable amounts of K but little Fe or Mg. Small pyrite grains are common inclusions in the clay. Accessory minor cementing phases are a fibrous or layered aluminosilicate zeolite, which forms radiating fans that grow off detrital minerals; several types of chalcedony; and asphalt. The chalcedony grows around quartz clasts with a cherty, pale brown and heavily zoned texture. Colloform chalcedony fills open space with at least two generations, both containing pyrite inclusions and crosscut by pyrite, carbonate, and asphalt veins.

Barite is locally abundant at Temple Mountain, but low in Sr. It forms overgrowths on K-feldspar and quartz, which have corroded edges at the contact. The barite at the Delta mine forms abundant euhedral laths disseminated through the host sandstone, in places forming concretions and overgrown by galena. No barite was observed at the Dirty Devil mine, but samples show gypsum overgrowing quartz overgrowths and possibly overgrowing the dolomite. The gypsum overgrows or veins all other phases in the rock and may be supergene.

Asphalt forms opaque, dark globules in interstices between grains. At the thin edges of the globules, it is translucent and dark brown, structureless, and not reflective. It is distinguished from epoxy by an S peak on EDS, and from plant coal by the lack of cellular structure and by decrepitating under the electron microprobe's beam. Asphalt globules contain roughly 1–10-micron-sized inclusions of pitchblende and bravoite, along with highly euhedral, fine-grained monazite, apatite, rutile, monazite, barite, and K-feldspar. Larger globules of asphalt are crosscut by the coarse cementing dolomite and overgrown by pyrite, and smaller asphalt globules are found as inclusions within the dolomite. All observed asphalt occurs outside quartz overgrowths, which are notably corroded at contacts (Fig. 7B). Previous studies have noted three types of asphalt in the San Rafael Swell deposits: uraniferous asphalt, non-uraniferous asphalt, and liquid petroleum [60, 65, 101].

As with the Big Indian deposits, the Chinle U-V deposits at the San Rafael Swell contain some uncommon authigenic minerals, including apatite, zircon, and monazite. Apart from the species forming inclusions under quartz overgrowths, Cl-rich apatite with chalcopyrite inclusions overgrows barite and galena at the Delta mine. Tiny apatite grains also form inclusions in asphalt. At Temple Mountain, a zircon crystal was found as a strikingly euhedral overgrowth on a heavily embayed quartz grain, both surrounded by asphalt. Monazite occurs as inclusions in asphalt and as an interstitial phase amid masses of pyrite surrounding quartz overgrowths.

Quartz overgrowths enclose lines of two-phase liquid–vapor fluid inclusions as well as the mineral inclusions.

Liquid–vapor inclusions are also found in the coarse cementing dolomite at the Dirty Devil and Lucky Strike mines; the carbonate cement at the Delta mine was found to contain liquid fluid inclusions with colorless, transparent daughter crystals.

#### 3.5.3 Metallic Mineralization

Pitchblende and uraniferous asphalt are reported by Hawley et al. [60] as the dominant ore minerals in these deposits. In this study, pitchblende was found only as tiny inclusions in blobs of asphalt (compositions verified by SEM–EDS) at Temple Mountain, and as inclusions under quartz overgrowths at Temple Mountain, Dirty Devil, and Delta. However, uraniferous asphalt was widely observed in the field around the deposits. Uranium also forms a U-V oxide of uncertain identity, possibly uvanite, at Temple Mountain. Montroseite was not observed, but a V-Cr-Fe oxide occurs as inclusions within asphalt at Temple Mountain. The majority of the V at least at Temple Mountain apparently forms vanadian phyllosilicates, which occur where the edges of quartz and other detrital grains are more than usually corroded. Its composition is that of a V-enriched muscovite or V-deficient roscoelite with detectable Mg, Fe, and Cr. Ningyoite is reported with pitchblende amid the asphalt at Temple Mountain, but was not observed in this study [101].

Pyrite is the most common base metal sulfide and multiple types exist: tiny inclusions in asphalt and under quartz overgrowths; freestanding grains overgrowing quartz overgrowths and sutures, and overgrown by the coarse dolomite cement; inclusions in chalcopyrite; and nodules engulfing detrital grains, which are very scarce and heavily corroded inside the pyrite nodule. Some of the pyrite inclusions under quartz overgrowths at the Delta mine appeared framboidal, although this identification is tentative. No detectable concentrations of metals other than Fe were detected in the pyrite at any location on the San Rafael Swell, although cattierite with variable Ni and Cu was identified among inclusions in the asphalt at Temple Mountain (Fig. 7, Table 3).

Chalcopyrite is common with brown chalcedony and as interstitial crystals amid the dolomite cement. At Delta, it forms inclusions within apatite grains. Covellite and digenite, or other Cu–S minerals with no Fe, were also possibly detected among the micron-scale inclusions in asphalt. At Dirty Devil, chalcopyrite is mixed with pyrite and bornite and overgrown by colloform chalcedony. It contains inclusions of pyrite and another opaque metallic phase tentatively identified as ferroselite.

Sphalerite occurs in two types, both of which form interstitial fillings. One is brown and transparent, probably corresponding to a cleophane composition with minor Cd, and forms coarse grains in interstices alongside chalcopyrite without a clear textural relationship. Marmatite is also present at Dirty Devil and overgrows chalcopyrite. At Temple Mountain, sphalerite was found only as inclusions under quartz overgrowths. Galena is common near pitchblende, including as microscopic grains in uraniferous asphalt. At the Delta mine, galena forms masses overgrowing barite laths, which remain euhedral and not visibly corroded. The galena is overgrown by Cl-rich apatite with chalcopyrite inclusions. Realgar was not observed in thin section, but was found in hand samples from near Temple Mountain.

Multiple types of hematite exist. Some of it surrounds and replaces pyrite, but tiny grains of hematite form inclusions under quartz overgrowths even in bleached and mineralized rocks. The replacive hematite tends to contain detectable Zn and Mn and variable Co. Hematite also forms concretions, some but not all of which pseudomorph pyrite nodules, at Temple Mountain, and occurs among the highly oxidized and colorful, probably supergene, mineral suite. Lermontovite or another U-phosphate, tyuyamunite, carnotite, and jarosite also occur overgrowing other alteration mineral phases.

### 3.6 Cutler Stratigraphically-Controlled Deposits

#### 3.6.1 Detrital

Ores are hosted in upper Cutler arkoses, composed mainly of quartz with accessory K-feldspar, albite, and lithic clasts and minor detrital biotite and phengite. Minor zircon is also present. Both quartz and feldspar grains are commonly corroded around the edges, with minor suturing. In mineralized samples, the biotite preserves a detrital appearance but contains detectable V.

#### 3.6.2 Alteration

Detrital felspar grains are veined by albite, which contains inclusions of pitchblende (Fig. 8C, E). The K-feldspar is strongly corroded in most samples. The principal cement in the rock is calcite, which contains inclusions of pyrite and pitchblende but has < 1 mass % Mn and little Fe. Three types of the chlorite are present: fans of Fe-dominated chlorite with low Mg and no V, surrounded by silica; K-bearing magnesian chlorite to biotite replacing detrital biotite, invaded along cleavages by U and V oxides; and fine-grained Mg-rich, Fe-poor authigenic chlorite or smectite with 0 to 5 mass % V and little to no K, fringing detrital grains and helping to cement the rock in mineralized areas. This last type of phyllosilicate is generally found where quartz overgrowths are heavily corroded or absent, with textures suggesting the chlorite/smectite replaced the quartz.

Some quartz overgrowths remain, though most are heavily corroded or crosscut by sutures between grains. Inclusions observed between rims and overgrowths are mainly

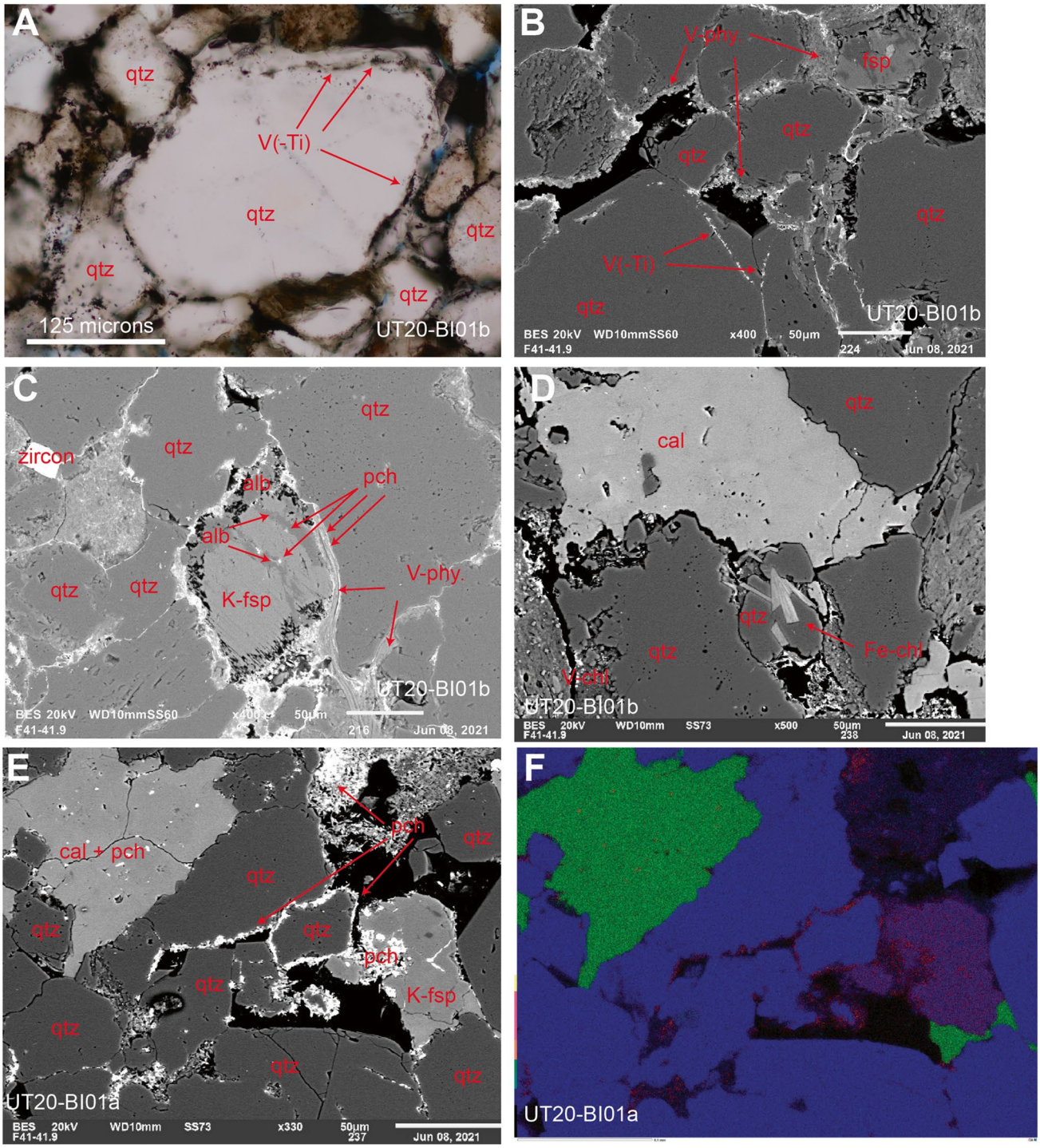


**Fig. 8** Minerals in stratigraphically controlled U-V ores in the Cutler, from the dumps of the reclaimed Big Buck (Cutler) mine. **A** Partially corroded quartz overgrowth enclosing lines of V(-Ti) oxide inclusions, transmitted ppl. Compare Figs. 4a and 5d. **B** SEM photomicrograph showing V phyllosilicates fringing corroded quartz grains, lines of V(-Ti) oxides in quartz, and the absence of overgrowths where V-phyllosilicates have developed. **C** Heavily altered detrital K-feldspar grain, overgrown by albite (alb) and veined by albite and pitchblende. Vanadian biotite, some of it derived from vanadization of detrital biotite, fringes quartz grains. SEM photomicrograph. **D** Calcite cement with pitchblende and pyrite inclusions (bright flecks) and two different types of authigenic phyllosilicates, vanadian (V-chl) and iron (Fe-chl) chlorites. SEM photomicrograph. **E** Fringes of pitchblende and V-phyllosilicates around detrital grains, and calcite with pitchblende inclusions. SEM photomicrograph. **F** Elemental RGB map of Si (blue), Ca (green), and U (red) of same field of view as in (**E**)

V-Ti oxides ranging in composition from V = Ti to V = 2Ti by weight, with detectable U (Table 5; Fig. 8B). Rarer species under quartz overgrowths include pyrite, montroseite, pitchblende, hematite, apatite, and Ti oxide without detectable V. In general, the pure Ti oxide grains occur in the middle parts of overgrowths rather than directly over the detrital cores. Less common overgrowths around albite typically contain hematite inclusions.

Zircon, while mainly detrital, is highly euhedral and shows strong zoning, which may point to authigenic growth. Grains of rutile and fluorapatite are present in quartz overgrowths but also occur as euhedral crystals within altered K-feldspar grains (rutile) and adjacent to quartz overgrowths (apatite), and may also be authigenic. Gypsum is rare but is found overgrowing pitchblende.

#### 3.6.3 Metallic Mineralization

Pitchblende is the main hypogene U mineral, forming rare inclusions under quartz overgrowths and more common fringes around clastic grains. It also invades detrital micas along cleavages and forms inclusions in the calcite, and is overgrown by the V-chlorite and in one sample by rare gypsum. Montroseite and other V-(hydr)oxides were observed only under quartz overgrowths; otherwise, the V observed occurs entirely in phyllosilicates. Most of the phyllosilicates consist of authigenic V-Mg chlorite.

Pyrite is common as inclusions in the calcite, along with pitchblende. No other metal sulfides or related minerals were observed with the exception of hematite, which occurs in sprays that may be specular. This is probably due to the small number of samples. Hematite was the only supergene phase identified, replacing pyrite.

#### 3.6.4 Cutler structurally-controlled deposits

*Detrital*: The host rock is an arkosic sandstone with grain size varying from fine to coarse. The main constituent is quartz, with abundant feldspar. While both tartan- and plagioclase-twinned varieties are common, SEM–EDS examination showed that potassic compositions heavily dominate, with much of the Na-rich plagioclase component replaced by K-feldspar. Both quartz and plagioclase grains are commonly shattered, and suturing is common between quartz grains. Especially at contacts with a cementing clay, the edges of quartz and feldspar grains are ragged. Muscovite and biotite are both present among the clastic grains. Detrital ilmenite grains are mostly replaced by rutile, and monazite has heavily corroded edges. Detrital zircon shows no evidence of corrosion, replacement, or authigenic growth. Coalified plant remains are uncommon but present and localize bleaching for up to several centimeters. Corey [90] reported detrital magnetite, chlorite, tourmaline, and chert and granite lithics, but these were not observed in this study.

#### 3.6.5 Alteration

Detrital muscovite is commonly altered to a kaolinitic clay around the edges, although biotite is largely unaltered. Feldspars are partly to completely altered to potassic compositions, with only minor remnant Na and no detectable Ca component. Unusually for Paradox Basin U-V deposits, no overgrowths around quartz or feldspar were observed for Cutler-hosted structurally controlled mineralization, nor have been reported in previous studies.

The major cements in the rock are calcite and an aluminous clay close to kaolinite in composition. The textural relationship between the two is unclear. In nearly all samples, the calcite lacks detectable Fe and has < 0.1 mass % Mn, but in one mineralized sample it is partially replaced by dolomite with several mass % Fe. In this sample, the dolomitization is adjacent to a veinlet of gypsum, which is otherwise not observed. The calcite fills vugs and forms concretions with large sparry crystals, but in most samples it is grungy-looking with fine to moderate grain sizes. Larger crystals of the calcite have noticeable inclusions of pyrite and are overgrown by a U-rich galena.

Barite is relatively common and has a very high Sr content, sometimes approaching 50% celestine; Davidson and Kerr [72] described it as "celestobarite." It overgrows the calcite, the quartz, and a highly zoned, U-rich galena, and contains inclusions of pyrite. Its relationship to the gypsum is uncertain as the two were not detected in the same samples. No apatite was observed but an unidentified interstitial Al-Sr phosphate overgrows the calcite. In addition to occurring as replacements for detrital ilmenite, rutile is found as a euhedral interstitial overgrowth on quartz. Asphalt was not definitively identified, but in bleached and/or mineralized samples there are common interstitial globules, dark and isotropic, with red internal reflections and C and S peaks on EDS. In the mineralized samples, such globules are commonly surrounded by grains of pitchblende, sulfide, and sulfate. This corresponds to descriptions of pyrobitumen in structurally controlled Cutler deposits by Corey [90].

Apart from those in detrital grains, fluid inclusions were not observed at the Atomic King mine.

#### 3.6.6 Metallic Mineralization

Pitchblende occurs along the rims of detrital grains along with rutherfordine, and as an interstitial local cement in relatively oxidized samples (Fig. 9C, D). Notably, it has a small but consistent V peak on EDS, corresponding to < 1 wt% V. The only other reduced U mineral found is rutherfordine, which forms inclusions in roscoelite and stubby brown

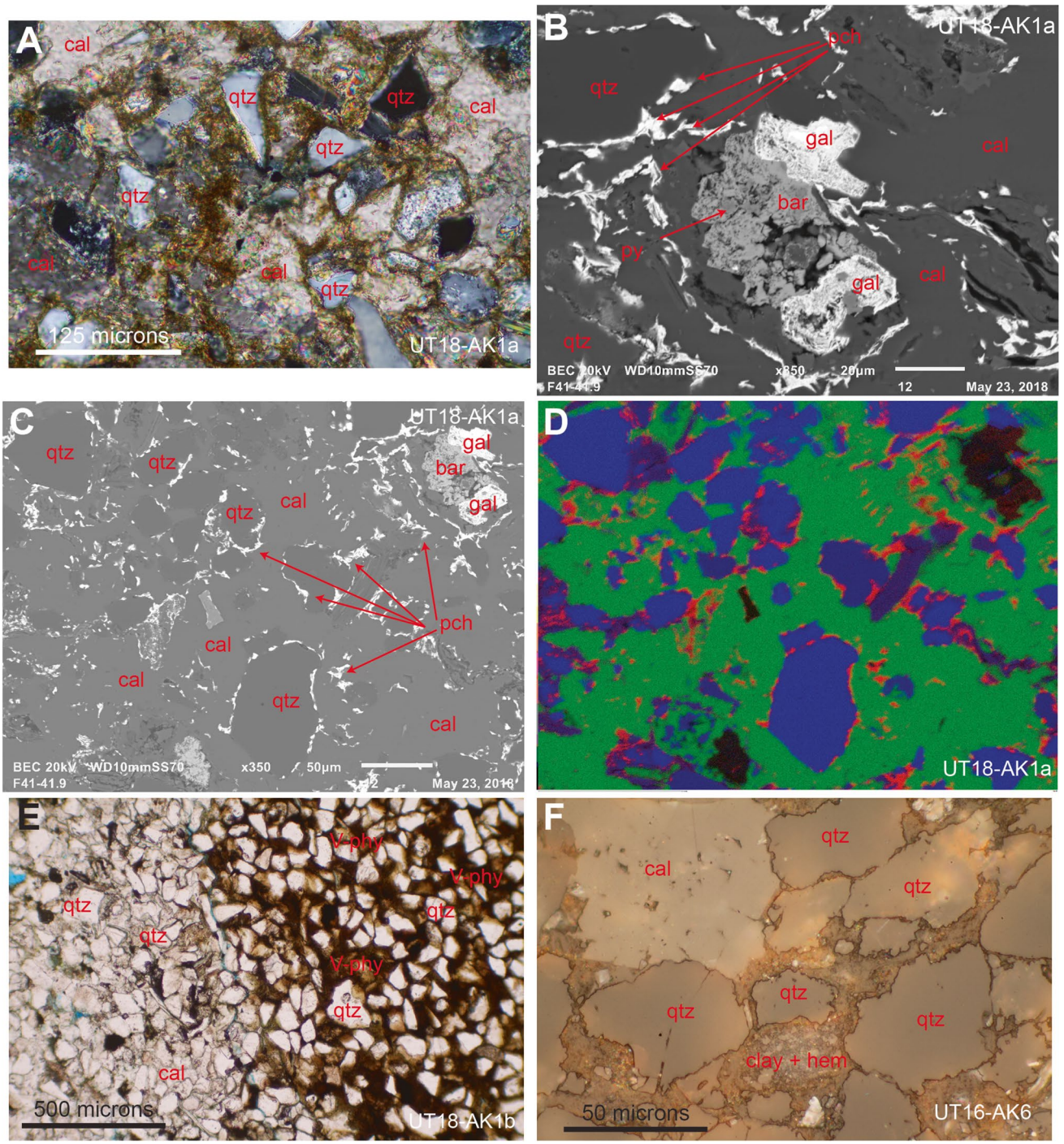


**Fig. 9** Ore and related alteration at the Atomic King mine, Cutler structure-hosted U-V deposit. **A** Low-grade V ore, showing V phyllosilicates as brown fringe around detrital quartz grains cemented by calcite, transmitted xpl. **B** SEM photomicrograph showing calcite cementing quartz fringed by pitchblende and overgrown by two generations of galena (inner solid and outer lacy), which in turn is overgrown by a barite that also contains pyrite inclusions. **C** SEM photomicrograph of ore texture similar to (**B**). **D** RGB elemental map of Si (blue), Ca (green), and U (red) of area in (**C**). **E** Sharp boundary between ore-bearing sandstone cemented by brown V-phyllosilicates and unmineralized, calcite-cemented rock; transmitted ppl. **F** Corrosion of detrital quartz grains amid hematitic, red-reflecting clay cement below coarse cementing calcite; reflected ppl

crystals fringing the edges of quartz grains, overgrown by calcite. Montroseite was not observed in this study but is reported in minute quantities by Corey [90] and Davidson and Kerr [72], typically as microscopic invasions along cleavages in detrital micas and as irregular masses in the pyrobitumen. Except for tyuyamunite and other vanadates, V was found only as a minor substituent in pitchblende and in phyllosilicates. The latter is mostly kaolinitic, with some roscoelite in ore zones. The roscoelite is an interstitial cement similar in texture and abundance to the kaolinite found in unmineralized samples. In contrast to textures observed in other Paradox Basin U-V deposit types, the edges of quartz and feldspar grains show no evidence of more than usual dissolution in contact with the roscoelite.

The most abundant accessory sulfide is pyrite, largely replaced by hematite but still visible as inclusions in roscoelite and calcite. Larger grains of pyrite are overgrown by the celestobarite, though the extent of replacement is unclear. Chalcopyrite is also common as fine grains growing off quartz rims, surrounded by pitchblende and calcite. In one sample, chalcopyrite is intergrown with pyrite and the two are overgrown by pitchblende around the edges. Corey [90] reports that chalcopyrite forms veins crosscutting pyrobitumen and uraninite, but this texture was not observed in the present study. Some of the chalcopyrite is partially replaced by digenite and covellite. Galena overgrows quartz and the calcite cement and is overgrown by the celestobarite. Backscatter and EDS analysis shows that the galena is heavily zoned into two distinct compositional types, with unremarkable PbS overgrown by an extremely U-enriched galena (Fig. 9B). Molybdenite and sphalerite are reported but were not observed (Table 3).

Hematite forms fine interstitial grains in light red rocks (Fig. 9E, F), probably those not bleached, but is also found replacing detrital biotite. At the sharp boundaries between red and white parts of the sandstone, hematite forms colloform concretions with highly reflective crystals in reflected light. Tyuyamunite and carnotite are the main supergene phases noted, forming wisps or flakes.

## 4 Paragenesis and Metallogenetic Implications

### 4.1 Paragenesis: Evaluation and Comparison with Previous Work

Five of the six deposit types in this study show strong similarities in mineralogy and textural relationships. All except the structurally controlled deposits in the Cutler Formation contain hematite inclusions, and sometimes rutile and barite, under quartz overgrowths (Table 5, Fig. 5H). These are strongly oxidized minerals and indicate that the host sandstones were originally red beds. Examples of all five types also contain one or more of pyrite, montroseite, and pitchblende under quartz overgrowths (Table 5; Fig. 4E, h; Fig. 5D, H; Fig. 6E, F; Fig. 7F; and Fig. 8A, B), making bleaching and mineralization the next events after reddening to leave visible traces in the rock. Bleaching of hematite-bearing red beds by sulfide-bearing fluids would have produced the pyrite. That pyrite occurs in the same paragenetic position as pitchblende and montroseite—under quartz overgrowths—suggests that mineralization began not long after bleaching, or perhaps was contemporaneous with it (Fig. 10). Findings such as the framboidal pyrite in Fig. 6G suggest a possible contribution from bacterial sulfate reduction. Other minerals also found under quartz overgrowths, including monazite, Ti oxides, and apatite, must also have precipitated at this time.

Most of the pitchblende and montroseite are pore-filling cements outside of quartz overgrowths (Fig. 4A, B; Fig. 5F; Fig. 6A–D; Fig. 7A, B; and Fig. 8A, E, F). In the Salt Wash and San Rafael Chinle-hosted deposits, both U and V minerals are found in structureless, commonly S-bearing organic matter that resembles asphalt under the microscope and appears to have eaten away nearby quartz grains (Fig. 4C, D and Fig. 7B). In the Chinle sandstone-hosted deposits, no asphalt was directly observed, but blue-fluorescing fluid inclusions in quartz indicate the presence of hydrocarbons [54]. Both pitchblende and montroseite are also found underneath and sometimes penetrating through quartz overgrowths (Fig. 4E–H, Fig. 5D, and Fig. 6E, F) in all except the structurally controlled Cutler deposits. In all deposits featuring overgrowths, the overgrowths are found heavily embayed or mostly dissolved where they are in contact with asphalt or V-phyllosilicates (Fig. 4F–H, Fig. 5F, G, Fig. 6C, Fig. 7B, and Fig. 8B, C. The V-phyllosilicates commonly form fringes that appear to replace preexisting overgrowths; Fig. 6C shows what looks like a reaction front where V-phyllosilicates (brown) have replaced quartz overgrowths and cement in the less-altered sandstone on the left side of the photomicrograph. Unlike pitchblende and montroseite, V-phyllosilicates have not been observed underneath or included within quartz overgrowths. The V-phyllosilicates also tend to form fringes around montroseite, as seen in Fig. 4C, D, where the two are in contact. This suggests that mineralization involved a main ore stage that precipitated pitchblende and montroseite starting before the quartz overgrowths formed, persisted through overgrowth formation, and ended afterwards (Fig. 10). This main ore stage would then have been followed by formation of V-phyllosilicates, either from a fresh influx of V or by back-reaction of newly formed montroseite with newly formed quartz overgrowths (as suggested by [102]). Either of these origins would be consistent with the textures observed in the rocks, and the two options are not mutually exclusive.

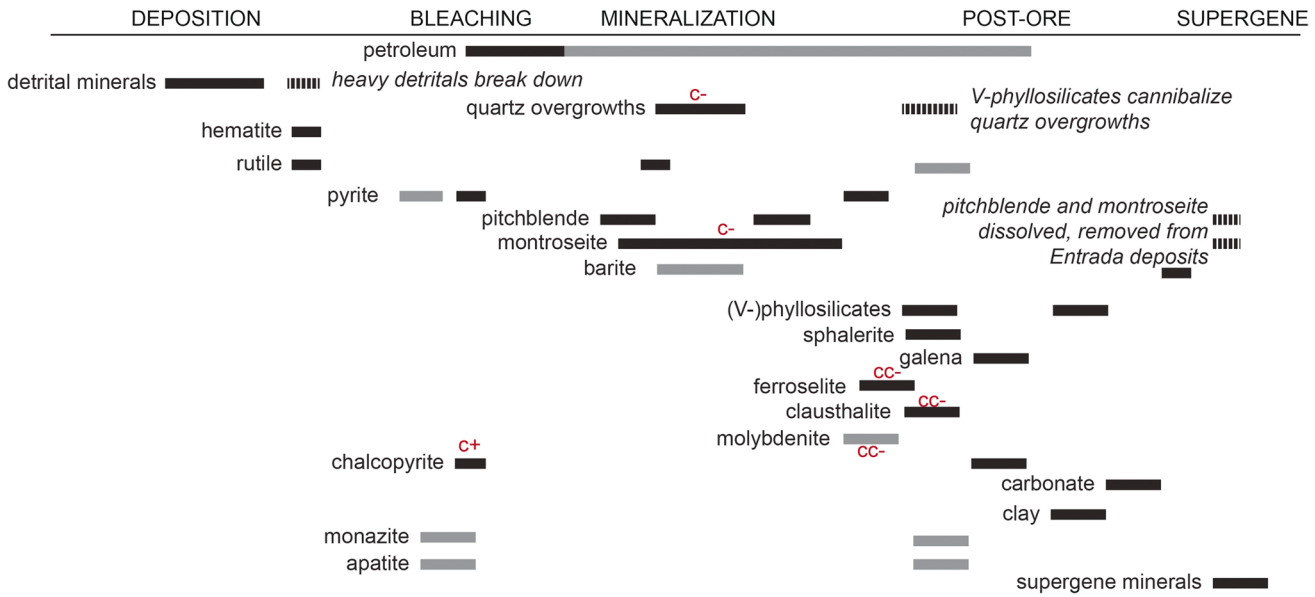


**Fig. 10** Interpreted timing of formation of minerals found in Paradox Basin U-V deposits, based on petrographic observations. Lines in black represent minerals whose textural position and timing are relatively well established from the data; those in gray represent paragenetic formation episodes whose timing can only be tentatively constrained. Dashed lines represent the dissolution or partial dissolution of minerals explained in the corresponding italic text. The paragenesis in this figure shows the order of formation of common minerals and significant accessory phases in all five deposit types considered. Exceptions are denoted by red annotations of "c−," meaning that there is no evidence for the formation of that mineral at that time in the structurally controlled Cutler-hosted U-V deposits, or "c+," meaning that that episode of mineral formation occurs only in the structurally controlled Cutler-hosted deposits. Annotations of "cc−" mean that the mineral formation episode is missing from both types of Cutler-hosted deposits and from the Big Indian Chinle deposits

**Table 6** Typical compositions of vanadian phyllosilicates at the sites in this study

| Deposit type | Location | V-phyllosilicate composition |
|---|---|---|
| Salt Wash | Pandora/Beaver | Mainly V-illite with minor Al-rich V-clinochlore with detectable Fe |
| | Legin group | Not observed |
| | Charles T group | Not observed |
| | Norma Jean #2 | Not observed |
| | Cougar group | V-clinochlore with detectable Fe overgrows roscoelite |
| | Van #4 | Roscoelite (probably) |
| | Unnamed rim cut, Monogram Mesa | Not observed |
| | Schoolmarm | V-clinochlore with detectable Fe |
| | Blue Streak | Magnesian V-chlorite with minor Fe, K-deficient V-biotite; rare V-illite or roscoelite |
| Entrada | Omega mines | End-member roscoelite |
| Chinle–Big Indian | Mi Vida | Ranges from roscoelite to V-clinochlore |
| | Serviceberry | V-chlorite and V-biotite |
| | Homestake | Composition not identified |
| | Big Buck | V-chlorite and V-biotite, highly magnesian |
| Chinle–San Rafael Swell | Temple Mountain | V-enriched muscovite (not roscoelite) with variable Mg, Fe, Cr |
| | Dirty Devil | Not observed |
| | Delta | Not observed |
| | Lucky Strike | Not observed |
| Cutler structure-related | Atomic King | Roscoelite |
| Cutler stratabound | Big Buck (Cutler) | Magnesian V-chlorite with minor K and Fe; V-biotite |

The compositions of the V-phyllosilicates also vary with the type of sandstone host. The clean quartzarenites of the Salt Wash and Entrada host the highest proportion of roscoelite and V-illite, whereas the arkosic Chinle and Cutler Formations contain more V-biotite and V-chlorite (Tables 1 and 6). The V-chlorite and V-biotite are consistently Mg-dominant in all deposit types where they occur.

The Salt Wash deposits contain accessory base-metal selenides (clausthalite, ferroselite), akin to more abundant base-metal sulfides (sphalerite, molybdenite, chalcopyrite) in the Chinle. These sulfides and selenides have textural relationships similar to the V-phyllosilicates. They occur outside the quartz overgrowths and overgrow montroseite or pitchblende, but are enclosed in cementing clays and carbonates. Paragenetic interpretation thus assigns them to the end of the ore stage (Fig. 10).

Except where U and V minerals fill the pores, most of the rocks are cemented by suturing between quartz overgrowths (Fig. 4E, g, Fig. 5F, Fig. 6E, F, Fig. 7A, and Fig. 8B, C) or by clay and/or a coarse-grained carbonate (Fig. 4H, Fig. 5A, B, E, Fig. 6C, H, Fig. 7C, and Fig. 8D–F). Clay and carbonate are also common cements in unmineralized rocks well away from the ore deposits [24, 41, 103, 104]. They may represent large-scale fluid movement and mixing in the Paradox Basin in general. At an unknown but late date, and likely continuing today, supergene alteration oxidized exposed metallic minerals to the colorful vanadate ores that first attracted attention to the U-V deposits on the Paradox Basin.

Our interpreted paragenesis varies somewhat across these five deposit types. In the Salt Wash and the Chinle Big Indian deposits, barite as well as hematite, pyrite, montroseite, and pitchblende is found under quartz overgrowths and sometimes penetrates all the way through them (Fig. 6E; Table 5). In both types, barite or celestine is also common as an accessory mineral outside the quartz overgrowths. It is overgrown by calcite and is partially replaced by the base-metal sulfides (e.g., Fig. 6B). This places barite in the same paragenetic position as the highly reduced hypogene U and V minerals (Fig. 10). This texture has not been observed in the other deposit types, though this may be due to the somewhat smaller number of unoxidized samples available from them.

The Entrada-hosted deposits are another variant on this theme. Evidence such as the vanadiferous pitchblende inclusions under quartz overgrowths suggests that interstitial pitchblende and montroseite were originally present in the deposit. Apart from the inclusions, these now exist only where they are encased in thick carbonate cement (Fig. 5D–F). The roscoelite that now dominates the ores shares the same texture as the V-phyllosilicates in the Salt Wash, Chinle, and stratigraphic Cutler deposits (Fig. 4H, Fig. 5G, and Fig. 6C), and like them appears to have cannibalized silica from the quartz overgrowths. It is speculative, but plausible, that the Entrada-hosted deposits once closely resembled those in the Salt Wash or at Big Indian. If this were the case, post-ore remobilization must have removed most of the original pitchblende and montroseite, leaving mainly the inclusions locked under quartz overgrowths and whatever V was locked in phyllosilicates notorious for insolubility [73]. In this interpretation, the Entrada-hosted deposits today are the residues left after original ores were remobilized and removed from the system.

The sixth deposit type, the U(-V) mineralization hosted in structures in the Cutler Formation, is distinct from the other five. This type lacks quartz overgrowths and contains pitchblende mainly as coatings around quartz grains (Fig. 9B–D), indicating that the quartz overgrowths shown in Fig. 10 failed to form. The pitchblende is instead overgrown by galena, pyrite, and barite, which are themselves overgrown by cementing calcite (Fig. 9A, B). This yields a paragenesis similar to the one in Fig. 10, with pitchblende forming during main-stage mineralization, followed by base-metal sulfides. However, quartz overgrowths and montroseite are missing. Mineralized hydrocarbons have been reported in other studies (Table 3 and references therein) but were not observed in this study.

### 4.2 Metallogenetic Implications

Some of the observations documented here have obvious implications for the origins of the U-V deposits in the Paradox Basin. Most notably, this work shows that there are more similarities than differences among the various types of U-V deposits in the Paradox Basin. While the macroscopic geological characteristics and the host rock lithologies vary, all six types are strikingly similar in mineralogy and textural relationships. The major U ore is pitchblende, and V mostly forms pore-filling montroseite or related V-oxides in all but the structure-controlled deposits in the Cutler formation and the Entrada-hosted ores. Vanadium phyllosilicates, mostly fringing quartz grains, are also significant contributors to the hypogene V resource in all six types of deposits. In the Entrada-hosted and structure-controlled Cutler deposits, where V-oxides are respectively absent and minor, phyllosilicates host practically all of the known V. The geological similarities across deposit types are also notable, particularly the exclusive occurrence of all U-V mineralization in light-colored sandstones that are elsewhere red. This correlation is so tight that bleaching of red beds was used as an exploration criterion by the USGS starting in the 1950s (e.g., [105, 106]). Tables 3 and 5 and Fig. 3J show clear evidence that the U-V deposits formed in sandstones that had been red and were bleached.

The geological and paragenetic similarities across deposit types have substantial implications for metallogenesis. Most

obviously, they imply that all but the structure-hosted Cutler deposits share a similar genesis. The likely outlines of this genesis include (1) bleaching by a reduced fluid; (2) oxidized fluids transporting U and V; and (3) ore precipitation by reduction either where the two fluids mixed or where the second fluid encountered rocks previously reduced by the first. The structure-controlled deposits in the Cutler likely formed by remobilization of overlying ores in the Chinle by oxidized waters, which reprecipitated their U and V where they encountered reduced rocks or fluid in the faults.

This interpreted metallogenesis, with some variations, has been the usual model for Paradox Basin U-V deposits for several decades now ([5, 34], this volume). However, the results of this study raise some new questions about its details. One is the role of hydrocarbons in ore formation, as either the reductants themselves or as reducing agents that bleached the rocks and prepared them to trap U and V. This is supported by the observation of mineralized relict hydrocarbons in the structure-controlled Cutler deposits [90], the San Rafael Swell Chinle deposits [85], and the Salt Wash deposits (Fig. 4C, D, F), and by the blue-fluorescing fluid inclusions in the Big Indian Chinle deposits [107]. No hydrocarbons have been definitively identified in the Entrada-hosted deposits in this or other studies, but much of the widespread bleaching in the Entrada is thought to result from hydrocarbon migration [108]. Lastly, compiled radiometric dates on the Paradox Basin U-V deposits show a peak between roughly 70 and 120 Ma (Fig. 11). These dates should be considered with caution for the reasons discussed by Ludwig et al. [109], but coincide well with the main phase of hydrocarbon generation based on Nuccio and Condon's [18] thermochronology.

A second new point from this study is the sheer extent of similarity across most of the deposits examined (Sect. 5.1). Some analogs between deposits had been noted before, going back to the mid-twentieth century. But the lack of overall synthesis and comparison across deposit types (noted in Sect. 1.2) tended to mask just how close the mineralogy and textural relationships are at most of the deposits. This is what makes it possible to interpret a general paragenesis (Fig. 10) applying to almost all of them. It also raises the question (previously touched on by Sanford's work) of whether all the Paradox Basin U-V deposits formed in a single basinwide mineralizing episode, or whether the ore-forming processes operated independently in different formations at different times.

The results of this study also point up the significance of V. The sandstone-hosted U endowment of the Paradox Basin is roughly comparable to that of worldwide equivalents like the Grants, Ordos, and Athabasca basins [112, 113]. Its contained V, however, has no known equivalent. In most Paradox Basin deposits V is more abundant than U (Table 1). The sole exceptions are the Chinle sandstone-hosted deposits in the White Canyon district, where V is not reported and Cu is the major accessory metal. However, in Big Indian, the same type of deposit contains abundant V. To make an analogy with another sediment-hosted system, vanadium is to the Paradox Basin what cobalt is to the Central African

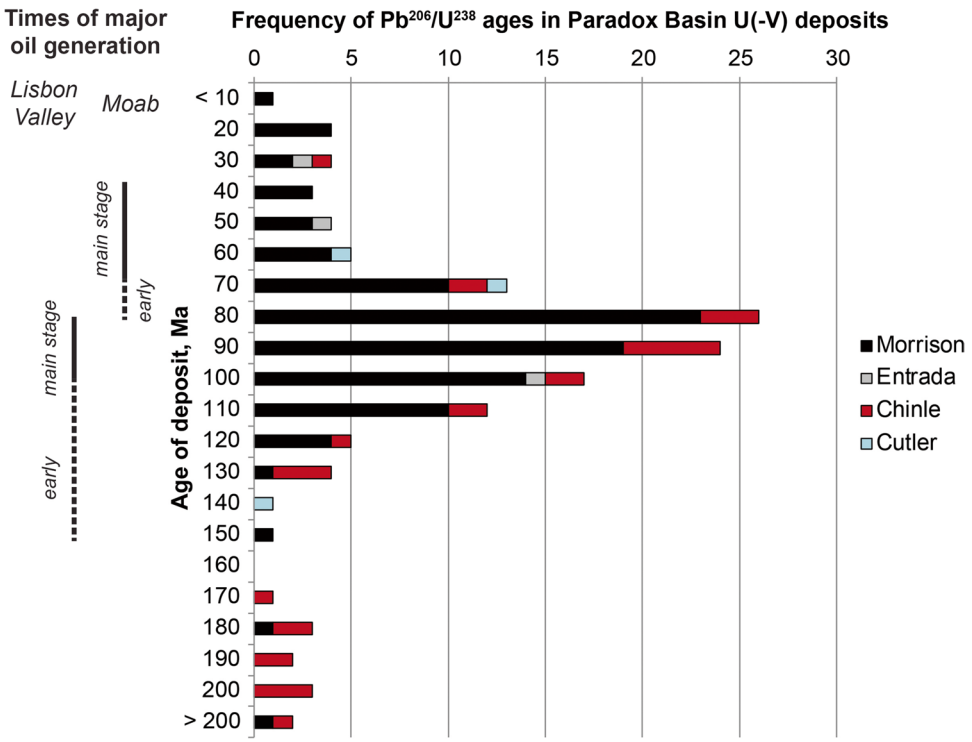


**Fig. 11** Histogram of ages obtained from U–Pb dating of U(-V) deposits on the Colorado Plateau, compared to oil generation windows from thermochronological work by Nuccio and Condon [18]. Dates are compiled from [71, 110, 111],and [109]

Copperbelt: an unexplained, world-class concentration of an element that in most deposits of that type is accessory at most. The current Paradox Basin metallogenetic model does not explain this world-class accumulation of V, without precedent in sandstone-hosted U provinces worldwide.

These questions—the role of hydrocarbons, the genetic relationship (or not) among deposit types, and the origins of the unparalleled V endowment—remain for future research on the Paradox Basin U-V deposits to resolve.

## 5 Conclusions

In the Paradox Basin, tabular deposits in the Salt Wash (Morrison) sandstone; lenticular deposits in the Entrada; stratabound deposits in the Chinle in the San Rafael Swell, White Canyon, and at the Chinle-Cutler unconformity at Big Indian; and stratabound deposits in the Cutler Formation in the Big Indian district, all share similar geological, mineralogical, and textural characteristics. Common features among five of these six include occurrence in red bed sandstones bleached during or slightly before the onset of mineralization; hypogene suites that are or were dominated by pitchblende and montroseite, and/or by V-phyllosilicates overgrowing them; inclusions of hematite, pyrite, and reduced U-V minerals under quartz overgrowths; accessory base metal sulfides and selenides overgrowing or crosscutting ore mineralization; traces of hydrocarbons; common framboidal pyrite and barite; authigenic rutile; extraordinary V concentrations; and a post-ore carbonate cement. (Deposits in the Entrada apparently once contained montroseite and pitchblende, which are now found only under quartz overgrowths.) A sixth type, structurally controlled deposits in the Cutler Formation, lacks quartz overgrowths and most of the montroseite, but is otherwise similar to the rest.

Textural relationships indicate that mineralization in the first five types of deposit began around the time of red bed bleaching (likely by hydrocarbons) or not long afterward, starting with pitchblende and montroseite, the earliest of which were overgrown by authigenic quartz. The V-phyllosilicates, which constitute a major proportion of the V resource in some of the deposits, formed later in the mineralizing episode, either by back-reaction of montroseite with silica from the quartz overgrowths or by reaction of silica with dissolved V. At this stage, base metal sulfides and selenides also precipitated, most commonly pyrite, chalcopyrite, and clausthalite, less commonly sphalerite, galena, ferroselite, molybdenite, and argentite/acanthite. Later fluids potentially unrelated to mineralization introduced carbonate and clay cements. Strongly oxidized surface waters converted much of the reduced U and V to supergene uranyl vanadates and related minerals. The deposits in the Entrada were remobilized completely except for V contained in insoluble V-phyllosilicates, and remnant montroseite and pitchblende under quartz overgrowths. Some of the Chinle ores were apparently remobilized downward into the underlying Cutler, precipitating at the hydrocarbon-bearing central zones of faults to create the sixth type of deposit.

This synthesis and comparison largely supports the existing model for U-V deposit formation in the Paradox Basin: reduction by a reducing fluid, followed by incursion of an oxidized, U-V-bearing water that precipitated the metals on contact with either this reducing fluid or the rocks that it bleached. However, it also trains a spotlight on features of the Paradox Basin U-V deposits that have not been fully explored or explained. One is the potential significance of hydrocarbons as ore-forming reductants. The second is the high level of mineralogical, textural, and paragenetic similarity across the sandstone-hosted U-V deposits in the Salt Wash, Entrada, Chinle, and much of the Cutler. These similarities could arise from deposit formation in a single basinwide ore-forming event, or from ore formation via the superposition of common geological processes (bleaching, mineralizing fluid incursion, precipitation) independently in different strata at different times. Lastly, this metallogenesis does not explain why the Paradox Basin—otherwise comparable to most sandstone-hosted U provinces worldwide—contains even more V than U. This remarkable V endowment sets the Paradox Basin apart from global equivalents.

**Supplementary Information** The online version contains supplementary material available at https://doi.org/10.1007/s42461-024-01128-6.

**Acknowledgements** This study was supported by US National Science Foundation grants #17-25338 and #20-45277 and by the W.M. Keck Foundation project "Evolution of Crustal Paleofluid Flow." We thank Kyle Kimmerle and Kyle Isenhart (independents), Daniel Kapostasy and Bruce Larson (Energy Fuels), and Craig Howell (Nuvemco) for mine access at Big Buck, Happy Jack, La Sal, and Blue Streak respectively. Craig also provided samples, geochemical data, and numerous helpful historical insights, as well as a field rescue. Jon Thorson contributed valuable time, guidance, and expertise. We appreciate these contributions and those of our collaborators at UA, especially Pete Reiners, Jason Kirk, Bob Krantz, Jennifer McIntosh, Eytan Bos Orent, Molly Radwany, Maxwell Drexler, George Davis, Amanda Hughes, and Ken Domanik. Comments from two anonymous reviewers greatly improved the manuscript. We further appreciate the contribution of the unnamed driver from Norwood who gave us a ride into Naturita, CO after a 10-mile night hike away from a field vehicle stuck in wet Mancos Shale in the Disappointment Valley in March of 2019. Whoever you are, thank you.

**Funding** National Science Foundation,20-45277,Isabel Barton,17-25338,Isabel Barton,W. M. Keck Foundation.

**Data Availability** Data will be provided upon request.

## Declarations

**Competing Interests** Author I. Barton is a member of the editorial board for *Mining*, *Metallurgy*, & *Exploration*.

## References


1. Kelley, K.D., Scott, C.T., Polyak, D.E., and Kimball, B.E., 2017. Vanadium. Chapter U in Scholtz, K., et al., eds., Critical Mineral Resources of the United States – Economic and Environmental Geology and Prospects for Future Supply, US Geological Survey Professional Paper 1802-U, 48 p.
2. Mudd GM, Jowitt SM, Werner TW (2016) The world's by-product and critical metal resources part 1: Uncertainties, current reporting practices, implications and grounds for optimism. Ore Geol Rev 86:924–938
3. Chenoweth, W.L., 2006. Lisbon Valley, Utah's largest uranium district. Mining Districts of Utah: Utah Geological Association, 534–550.
4. Cuney M (2009) The extreme diversity of uranium deposits. Miner Deposita 44:3–9
5. Barton IF (2024) Paradox basin uranium-vanadium deposits: History and significance of geological research. Min Metall Explor 41(4):1659–1676. https://doi.org/10.1007/s42461-024-01025-y
6. Kerr PF (1958) Uranium emplacement in the Colorado Plateau. GSA Bull 69:1076–1112
7. Sanford RF (1982) Preliminary model of regional Mesozoic groundwater flow and uranium deposition in the Colorado Plateau. Geology 10:348–352
8. Sanford RF (1992) A new model for tabular-type uranium deposits. Econ Geol 87:2041–2055
9. Sanford RF (1994) A quantitative model of ground-water flow during formation of tabular sandstone uranium deposits. Econ Geol 89:341–360
10. Hall SM, Van Gosen BS, Zielinski RA (2023) Sandstone-hosted uranium deposits of the Colorado Plateau, USA. Ore Geol Rev 155:105353
11. Barbeau DL (2003) A flexural model for the Paradox Basin: implications for the tectonics of the Ancestral Rocky Mountains. Basin Res 15(1):97–115
12. Hite, R.J., Anders, D.E., and Ging, T.G., 1984. Organic-rich source rocks of Pennsylvanian age in the Paradox Basin of Utah and Colorado. Hydrocarbon Source Rocks of the Greater Rocky Mountain Region, Rocky Mountain Association of Geologists, 255–2xx.
13. Hintze, L., and Kowallis, B., 1988. Geological history of Utah. Brigham Young University, 202 p.
14. Trudgill BD (2011) Evolution of salt structures in the northern Paradox Basin: controls on evaporite deposition, salt wall growth and supra-salt stratigraphic architecture. Basin Res 23:208–238
15. Flowers RM, Wernicke BP, Farley KA (2008) Unroofing, incision, and uplift history of the southwestern Colorado Plateau from apatite (U-Th)/He thermochronometry. GSA Bull 120(5–6):571–587
16. Murray KW, Reiners PW, Thomson SN (2016) Rapid Pliocene-Pleistocene erosion of the central Colorado Plateau documented by apatite thermochronology from the Henry Mountains. Geology 44(6):483–486
17. Baars DL (2000) The Colorado Plateau: a geologic history. University of New Mexico Press, Albuquerque, NM, p 254
18. Nuccio, V., and Condon, S., 1996. Burial and thermal history of the Paradox Basin, Utah and Colorado, and petroleum potential of the Middle Pennsylvanian Paradox formation. USGS Bulletin 2000-O, 47 p.
19. Blakey, R.C., and Ranney, W., 2008. Ancient Landscapes of the Colorado Plateau. Grand Canyon Association, AZ: 156 p.
20. Sprinkel, D.A., Chidsey, T.C., and Anderson, P.B., eds., 2010. Geology of Utah's Parks and Monuments. Utah Geological Association Publication 28: 623 p.
21. Kim JH, Bailey L, Noyes C, Tyne RL, Ballentine CJ, Person M, Ma L, Barton MD, Barton IF, Reiners PW, Ferguson G, McIntosh J (2022) Hydrogeochemical evolution of formation waters responsible for sandstone bleaching and ore mineralization in the Paradox Basin, Colorado Plateau, USA. Geol Soc Am Bull 134(9–10):2589–2610
22. Clem, K.M., and Brown, K.W., 1984. Petroleum resources of the Paradox Basin. Utah Geological Survey Report 119: 166 p.
23. Beitler B, Chan M, Parry T (2003) Bleaching of Jurassic Navajo Sandstone on Colorado Plateau Laramide highs: evidence of exhumed hydrocarbon supergiants? Geology 31(12):1041–1044
24. Loope D, Kettler R, Weber K (2010) Follow the water: connecting a $CO_2$ reservoir and bleached sandstone to iron-rich concretions in the Navajo Sandstone of south-central Utah, USA. Geology 38(11):999–1002
25. Loope DB, Kettler RM (2015) The footprints of ancient $CO_2$-driven flow systems: Ferrous carbonate concretions below bleached sandstone. Geosphere 11(3):943–957
26. Thorson, J.P., 2004, Paradox Basin sandstone-hosted copper deposits generated by two episodes of basinal fluid expulsion [abst]: Geological Society of America Abstracts with Programs, v. 36, p517.
27. Shope, C.L., and Gerner, S.J., 2014. Assessment of dissolved-solids loading to the Colorado River in the Paradox Basin between the Dolores River and Gypsum Canyon, Utah. US Geological Survey Scientific Investigations Report 2014–5031.
28. Carter, W., and Gualtieri, J., 1965. Geology and uranium-vanadium deposits of the La Sal quadrangle, San Juan County, Utah, and Montrose County, Colorado. USGS PP 508.
29. Shawe D, Archbold N, Simmons G (1959) Geology and uranium-vanadium deposits of the Slick Rock district, San Miguel and Dolores counties, Colorado. Econ Geol 54:395–415
30. Shawe, D., 1968. Petrography of sedimentary rocks in the Slick Rock district, San Miguel and Dolores Counties, Colorado. US Geological Survey Professional Paper 576-B, 41 p.
31. Shawe, D., 1976. Sedimentary rock alteration in the Slick Rock district, San Miguel and Dolores counties, Colorado. USGS PP 576-D, 58 p.
32. Shawe, D., 2011. Uranium-vanadium deposits of the Slick Rock district, Colorado. USGS PP 576-F, 89 p.
33. Northrop H, Goldhaber M (1990) Genesis of the tabular-type vanadium-uranium deposits of the Henry basin. Utah Economic Geology 85(2):215–269
34. Northrop H, Goldhaber M, Landis G, Unruh J (1990) Part I. Geochemical and mineralogical evidence for the sources of the ore-forming fluids. Econ Geol 85(2):215–269
35. Johnson, H.S., and Thordarson, W., 1966. Uranium deposits of the Moab, Monticello, White Canyon, and Monument Valley Districts, Utah and Arizona. US Geological Survey Bulletin 1222-H, 59 p.
36. Dalrymple, J.W., Dickinson, R.C., and Young, N.B., 1957. Environment of uranium deposition in the Bull Canyon area, Southwestern Colorado. US Atomic Energy Commission Report RME-103, 38 p.
37. Phoenix DA (1958) Uranium deposits under conglomeratic sandstone of the Morrison formation, Colorado and Utah. GSA Bull 69:403–418

38. Weeks, A., Coleman, R., and Thompson, M., 1959. Summary of the ore mineralogy. In Garrels, R., and Larsen, E., eds., Geochemistry and mineralogy of the Colorado Plateau uranium ores, USGS PP 320: 65–80.
39. Rohl, A.N., 1985. Alteration and mineralization in the Uravan mineral belt, Colorado. Unpublished Ph.D. dissertation, Columbia University, 171 p.
40. Fischer, R.P., 1955. Regional relations of the vanadium-uranium-chromium deposits in the Entrada sandstone, western Colorado. US Geological Survey Trace Elements Memorandum Report 916: 21 p.
41. Garden IR, Guscott SC, Burley SD, Foxford KA, Walsh JJ, Marshall J (2001) An exhumed paleo-hydrocarbon migration fairway in a faulted carrier system, Entrada Sandstone of SE Utah, USA. Geofluids 1:195–213
42. Allen MA, Butler GM (1921) Vanadium. University of Arizona Bulletin: Mineral Technology Series 26:1–23
43. Haff JC (1944) Petrology of two clastic dikes from the Placerville district. Colorado American Journal of Science 242(4):204–217
44. Hess, F.L., 1912. Vanadium deposits in Colorado, Utah, and New Mexico. US Geological Survey Bulletin 530-K, 31 p.
45. Breit GN (1995) Origin of clay minerals associated with V-U deposits in the Entrada sandstone, Placerville mining district, southwestern Colorado. Econ Geol 90:407–419
46. Lindgren W (1919) Mineral Deposits, 2nd edn. McGraw-Hill, New York, pp 407–412
47. Trites, A.F., and Chew, R.T., 1955. Geology of the Happy Jack mine, White Canyon area, San Juan County, Utah. US Geological Survey Bulletin 1009-H: 235–248.
48. Wengerd SA, Strickland JW (1954) Pennsylvanian stratigraphy of Paradox salt basin, Four Corners region, Colorado and Utah. AAPG Bulletin 38(10):2157–2199
49. Huber, G., 1980. Stratigraphy and uranium deposits, Lisbon Valley district, San Juan County, Utah. Quarterly of the Colorado School of Mines 75.2, 51 p.
50. Miller LJ (1955) Uranium ore controls of the Happy Jack deposit, White Canyon, San Juan County, Utah. Econ Geol 50:156–169
51. Lekas, M.A., and Dahl, H.M., 1956. The geology and uranium deposits of the Lisbon Valley Anticline, San Juan County, Utah. Intermountain Association of Petroleum Geologists 7th Annual Field Conference, 161–168.
52. Loring, W., 1958. Geology and ore deposits of the northern part of the Big Indian district, San Juan County, Utah. Unpublished Ph.D. thesis, University of Arizona, 1958.
53. Puffett, W.P., and Weir, G.W., 1959. Geological investigations of radioactive deposits semiannual progress report. USGS Trace Elements Investigations report 752, 131 p.
54. Barton IF, Barton MD, Thorson JP (2018) Characteristics of Cu and U-V deposits in the Paradox Basin (Colorado Plateau) and associated alteration. Society of Economic Geologists Guidebook Series 59:73–102
55. Wood, H.B., 1968. Geology and exploitation of uranium deposits in the Lisbon Valley area, Utah. In: Ridge, J.D., ed., Ore Deposits of the United States, 1933–1967: American Institute of Mining Engineers, New York, NY: 771–789.
56. Isachsen YW (1954) Ore deposits of the Big Indian Wash-Lisbon Valley area. In Guidebook to the Geology of Utah 9:95–106
57. Weir, G., and Puffett, W., 1981. Incomplete manuscript on stratigraphy and structural geology and uranium-vanadium and copper deposits of the Lisbon Valley area, Utah-Colorado. USGS OFR 81–39.
58. Schmitt, L.J., 1968. Uranium and copper mineralization in the Big Indian Wash-Lisbon Valley mining district, southeastern Utah. Unpublished Ph.D. thesis, Columbia University, 188 p.
59. Kennedy, V.C., 1961. Geochemical studies of mineral deposits in the Lisbon Valley Area, San Juan County, Utah. Unpublished Ph.D. dissertation, University of Colorado-Boulder, 254 p.
60. Hawley, C.C., Robeck, R.C., and Dyer, H.B., 1968. Geology, altered rocks, and ore deposits of the San Rafael Swell, Emery County, Utah. US Geological Survey Bulletin 1239: 121 p.
61. Robeck, R.C., 1954. Uranium deposits of Temple Mountain. Intermountain Association of Petroleum Geologists Fifth Annual Field Conference: 110–111.
62. Keys, W.S., 1954. The Delta mine, San Rafael Swell, Emery County, Utah. US Atomic Energy Commission report RME-59, 32 p.
63. Wright R (1955) Ore controls in sandstone uranium deposits of the Colorado Plateau. Econ Geol 50:135–155
64. Kerr PF, Bodine MW, Kelley DR, Keys WS (1957) Collapse features, Temple Mountain uranium area, Utah. GSA Bull 68:933–962
65. Kelley DR, Kerr PF (1958) Urano-organic ore at Temple Mountain, Utah. GSA Bull 69:701–756
66. Dix, G.P., 1954. The uranium deposits of Big Indian Wash, San Juan County, Utah (revised edition). US Atomic Energy Commission report RME-4022, 17 p.
67. Campbell, J.A., and Steele-Mallory, B.A., 1979. Uranium in the Cutler formation, Lisbon Valley, Utah. In: Baars, D.L., ed., Permianland: a field symposium/guidebook. Four Corners Geological Society, 23–32.
68. Reynolds R, Hudson M, Fishman N, Campbell J (1985) Paleomagnetic and petrologic evidence bearing on the age and origin of uranium deposits in the Permian Cutler Formation, Lisbon Valley, Utah. GSA Bull 96:719–730
69. Jacobs, M.B., 1963. Alteration studies and uranium emplacement near Moab, Utah: Part 1: Hydrothermal alteration along the Lisbon Valley Fault Zone, San Juan County, Utah. Part 2: Alteration studies of Cutler and Chinle strata along Lisbon Valley anticline, San Juan County, Utah. Unpublished Ph.D. thesis, Columbia University, 227 p.
70. Beahm, D.L., and Hutson, H.J., 2007. Velvet mine uranium project, San Juan County, Utah. NI43–101 Mineral Resource Report, 39 p.
71. Berglof, W., 1970. Absolute age relationships in selected Colorado Plateau uranium ores. Unpublished Ph.D. thesis, Columbia University, 149 p.
72. Davidson D, Kerr P (1968) Uranium-bearing veins in Plateau strata, Kane Creek, Utah. GSA Bull 79:1503–1526
73. Radwany MR, Barton IF (2022) The process mineralogy of leaching sandstone-hosted uranium-vanadium ores. Miner Eng 187:107811
74. Drexler M, Barton IF, Zanetta PM (2023) Vanadium in phyllosilicate ores: occurrence, crystal chemistry, and leaching behavior. Miner Eng 201:108205
75. Garrels, R., and Larsen, E., eds., 1959. Geochemistry and mineralogy of the Colorado Plateau uranium ores, USGS PP 320: 157–164.
76. Garrels, R., Larsen, E., Pommer, A., and Coleman, R., 1959. Detailed chemical and mineralogical relations in two vanadium-uranium ores. In Garrels, R., and Larsen, E., eds., Geochemistry and mineralogy of the Colorado Plateau uranium ores, USGS PP 320: 165–184.
77. Kampf AR, Hughes JM, Marty J, Nash BP, Chen YS, Steele IM (2015) Bluestreakite, $K_4Mg_2(V^{4+}{}_2V^{5+}{}_8O_{28})*14H_2O$, a new mixed-valence decavanadate mineral from the Blue Streak mine, Montrose County, Colorado: Crystal structure and descriptive mineralogy. Can Mineral 52:1007–1018
78. Roach, C.H., and Thompson, M.E., 1959. Sedimentary structures and localization and oxidation of ore at the Peanut mine, Montrose County, Colorado. In Garrels, R., and Larsen, E., eds.,

Geochemistry and mineralogy of the Colorado Plateau uranium ores, USGS PP 320: 197–202.
79. Spirakis CS (1977) The role of semipermeable membranes in the formation of certain vanadium-uranium deposits. Econ Geol 72:1442–1448
80. Fischer RP (1937) Sedimentary deposits of copper, vanadium-uranium and silver in southwestern United States. Econ Geol 32:906–951
81. Hess FL (1914) A hypothesis for the origin of the carnotites of Colorado and Utah. Econ Geol 9:675–688
82. Notestein FB (1918) Some chemical experiments bearing on the origin of certain uranium-vanadium ores. Econ Geol 13:50–64
83. Gross E (1956) Mineralogy and paragenesis of the uranium ore, Mi Vida mine, San Juan County, Utah. Econ Geol 51:632–648
84. Coleman RG, Delevaux M (1957) Occurrence of selenium in sulfides from some sedimentary rocks of the western United States. Econ Geol 52:499–527
85. Kelley DR, Kerr PF (1957) Clay alteration and ore, Temple Mountain, Utah. GSA Bull 68:1101–1116
86. Abdel-Gawad AM, Kerr PF (1973) Alteration of Chinle siltstone and uranium emplacement, Arizona and Utah. Geol Soc Am Bull 74:23–46
87. Hausen DM (1956) Paragenesis of the Temple Mountain uraniferous asphaltites. Geol Soc Am Bull 67(12):1795
88. Hawley, C.C., Wyant, D.G., and Brooks, D.B., 1965. Geology and uranium deposits of the Temple Mountain district, Emery County, Utah. US Geological Survey Bulletin 1192: 162 p.
89. Jensen ML (1958) Sulfur isotopes and the origin of sandstone-type uranium deposits. Econ Geol 53:598–616
90. Corey, A.S., 1959. Mineralogy and petrology of the uranium deposits of Cane Springs Canyon, San Juan and Grand Counties, Utah. US Atomic Energy Commission report RME-128, 65 p.
91. Hayes T (1982) Climate dependent geochemical mechanisms of copper, uranium, and vanadium transport and deposition in sandstone ores. Unpublished M.S. thesis, Stanford University, p 148
92. Elston, D.P., and Botinelly, T., 1959. Geology and mineralogy of the J.J. mine, Montrose County, Colorado. In: Garrels, R., and Larsen, E., eds., Geochemistry and mineralogy of the Colorado Plateau uranium ores, USGS PP 320: 213–218.
93. Archbold NL (1959) Relationship of carbonate cement to lithology and vanadium-uranium deposits in the Morrison formation in southwestern Colorado. Econ Geol 54:666–682
94. Brooks, R.A., and Campbell, J.A., 1976. Preliminary investigation of the elemental variation and diagenesis of a tabular uranium deposit, La Sal mine, San Juan County, Utah. US Geological Survey Open-File Report 76–287, 34 p.
95. Radwany, M.R., 2021. Geometallurgical characterization of sandstone-hosted vanadium ore from the Colorado Plateau. Unpublished M.S. thesis, University of Arizona, 57 p.
96. Evans, H.T., 1959. The crystal chemistry and mineralogy of vanadium. In: Garrels, R., and Larsen, E., eds., Geochemistry and mineralogy of the Colorado Plateau uranium ores, USGS PP 320: 91–102.
97. Foster, M.D., 1959. Chemical study of the mineralized clays. In: Garrels, R., and Larsen, E., eds., Geochemistry and mineralogy of the Colorado Plateau uranium ores, USGS PP 320: 121–132.
98. Zanetta PM, Drexler MS, Barton IF, Zega TJ (2023) Vanadium electronic configuration determination from $L_{2,3}$ transition in V-oxide compounds and roscoelite. Microsc Microanal 29(2):459–469
99. Merin IS, Segal DB (1989) Diagenetic alteration of the Wingate Formation: possible indications of hydrocarbon microseepage, Lisbon Valley, Utah. J Geol 976:719–734
100. Barton PB, Toulmin P (1966) Phase relations involving sphalerite in the Fe-Zn-S system. Econ Geol 61:815–849
101. Parnell J, Eakin P (1987) The replacement of sandstones by uraniferous hydrocarbons: significance for petroleum migration. Mineral Mag 51:505–515
102. Meunier JD (1994) The composition and origin of vanadium-rich clay minerals in Colorado Plateau Jurassic sandstone. Clays Clay Miner 42(4):391–401
103. Pearce JM, Kirby GA, Lacinska A, Bateson L, Wagner D, Rochelle CA, Cassidy M (2011) Reservoir-scale $CO_2$-fluid rock interactions: preliminary results from field investigations in the Paradox Basin, southeast Utah. Energy Procedia 4:5058–5065
104. Eichhubl P, Davatzes NC, Becker SP (2009) Structural and diagenetic control of fluid migration and cementation along the Moab Fault, Utah. AAPG Bulletin 93(5):653–681
105. McKay, E.J., 1955. Criteria for outlining areas favorable for uranium deposits in parts of Colorado and Utah. US Geological Survey Bulletin 1009-J, 282 p.
106. Weir, D.B., 1952. Geologic guides to prospecting for carnotite deposits on Colorado Plateau. US Geological Survey Bulletin 988-B, 15–27.
107. Barton MD, Barton IF, Thorson JP (2018) Paleofluid flow in the Paradox Basin: introduction. Society of Economic Geologists Guidebook Series 59:1–12
108. Bailey LR, Drake H, Whitehouse MJ, Reiners PW (2022) Characteristics and consequences of hydrocarbon migration: a natural example from the Entrada Sandstone, southern Utah. Geochem Geophys Geosyst 23(8):e2022GC101465
109. Ludwig K, Simmons K, Webster J (1984) U-Pb isotope systematics and apparent ages of uranium ores, Ambrosia Lake and Smith Lake districts, Grants mineral belt, New Mexico. Econ Geol 79:323–337
110. Miller DS, Kulp JL (1963) Isotopic evidence on the origin of the Colorado Plateau uranium ores. Geol Soc Am Bull 74:609–630
111. Stieff, L.R., Stern, T.W., and Milkey, R.G., 1953. A preliminary determination of the age of some uranium ores of the Colorado Plateaus by the lead-uranium method. US Geological Survey Circular 271: 19 p.
112. Dahlkamp F (2009) Uranium deposits of the world: USA and Latin America. Springer-Verlag, Berlin, p 536
113. Kyser, K., 2014. Uranium ore deposits. Treatise on Geochemistry 2nd ed., 13: 489–513.

## Authors and Affiliations

**Isabel Barton**[1] · **Mark Barton**[2,3]

✉ Isabel Barton
fay1@email.arizona.edu

[1] Department of Mining and Geological Engineering, University of Arizona, Tucson, USA

[2] Department of Geosciences, University of Arizona, Tucson, USA

[3] Lowell Institute for Mineral Resources, University of Arizona, Tucson, USA